Journal of Constructional Steel Research 226 (2025) 109254

Contents lists available at ScienceDirect

Journal of Constructional Steel Research

journal homepage: www.elsevier.com/locate/jcsr

Design provision assessment for the resistance of laterally restrained cellular steel beams

Vitaliy V. Degtyarev [a], Stephen J. Hicks [b,*], Felipe Piana Vendramell Ferreira [c], Konstantinos Daniel Tsavdaridis [d]

[a] New Millennium Building Systems, LLC, 3700 Forest Dr. Suite 501, Columbia, SC 29204, United States of America
[b] School of Engineering, University of Warwick, Coventry, CV4 7AL, United Kingdom
[c] Faculty of Civil Engineering – Campus Santa Mônica, Uberlândia, Federal University of Uberlândia, Minas Gerais, Brazil
[d] Department of Engineering, School of Science and Technology, City, University of London, Northampton Square, London, EC1V 0HB, United Kingdom

ARTICLE INFO

Dataset link: Database of the uniform ultimate l oads applied to laterally restrained cellular stee l beams (Original data)

Keywords:
Cellular beams
Lateral restraint
Resistance
Numerical simulations
Reliability
Design provisions

ABSTRACT

This paper evaluates the accuracy and reliability of laterally restrained cellular beams designed according to SCI P355, EN 1993-1-13, and AISC Design Guide 31 (DG31). The evaluations relied on extensive numerical data developed within the study using FE models validated against test results. The reliability analyses followed EN 1990 Annex D for both SCI P355 and EN 1993-1-13, and AISI S100 Chapter K for AISC DG31. The improved Hasofer–Lind–Rackwitz–Fiessler (iHL–RF) reliability method was also used for all considered provisions. The results indicate that SCI P355 and EN 1993-1-13 predict the beam resistance reasonably well, while AISC DG31 produces higher mean and coefficient of variation values of the simulation-to-prediction ratios than the European provisions. Partial factors computed per EN 1990 Annex D exceeded 1.00 for many failure modes, but the iHL–RF method indicated that the partial factor of 1.00 is justified for all limit states except for web-post buckling determined according to EN 1993-1-13. These results demonstrate that the EN 1993-1-13 web-post buckling rules should be revised and the more onerous buckling curve *c* used in design. Whilst this proposed change may be considered controversial for such a new standard, buckling curve *c* has been widely used in design according to SCI P355 for 15 years. AISC DG31 produced conservative designs. The findings of this study highlight areas where the existing provisions need revision and provide insights on how the improvements can be made, thereby contributing to the safety and economy of this form of construction.

1. Introduction

Cellular steel beams, defined as steel beams with regularly spaced circular web openings, are often used in construction due to their lightweight, long-span capabilities, and the ability to integrate services within the structural floor depth [1,2]. These structural benefits come at the cost of more complex design, with the need to consider multiple failure modes. The presence of closely spaced web openings not only affects the resistances typically considered in the design of steel beams with solid webs (including lateral–torsional buckling (LTB), beam global bending (BGB), and shear (BGS)), but also introduces additional failure modes requiring appropriate analysis and design, such as Vierendeel bending of the Tees (VBT), web-post shear (WPS), and web-post buckling (WPB).

Many researchers have studied the behavior and resistance of cellular beams experimentally and numerically. Results of experimental studies of cellular beams exhibiting various failure modes can be found in the following publications: BGB [3], VBT [3–6], WPS [4], WPB [4–9], and LTB [5,9–11]. It should be noted that the experimental studies involved cellular beams with relatively short spans, some of which were intentionally designed to provoke specific failure modes, while others aimed at exploring possible failure modes.

The recent developments in computational methods, advanced structural analysis software, and computational power, combined with the significant interest in this topic from researchers, produced many finite element (FE) numerical studies devoted to the behavior and resistance of cellular beams [6–9,12–20]. It should be noted that practically all numerical studies considered either laterally unrestrained beams [6,8,9,12–19] or restrained beams with relatively short spans [19,20].

The results of the experimental and numerical studies laid the basis for the European and North American design provisions developed

* Corresponding author.
E-mail addresses: vitaliy.degtyarev@newmill.com (V.V. Degtyarev), stephen.j.hicks@warwick.ac.uk (S.J. Hicks), fpvferreira@ufu.br (F.P.V. Ferreira), konstantinos.tsavdaridis@city.ac.uk (K.D. Tsavdaridis).

https://doi.org/10.1016/j.jcsr.2024.109254
Received 3 April 2024; Received in revised form 21 November 2024; Accepted 5 December 2024
Available online 17 December 2024

over several years, including SCI P100 [21], ENV 1993-1-1: 1992/A2: 1998 [22], SCI P355 [1], EN 1993-1-13 [23], and AISC Design Guide 31 (AISC DG31) [2]. The design provisions are mostly based on the research that studied the local failure modes (VBT, WPS, and WPB) or LTB of unrestrained beams, while the BGS and BGB failure modes have not been studied extensively. In reality, cellular beams are often laterally restrained by steel decking when it is orientated transversely and attached to the compression flange [2,24], which eliminates the LTB failure mode and may result in complex beam behavior, affecting the beam's resistance. The absence of the LTB failure mode allows for longer beam spans with a higher potential for the interaction of different failure modes caused by internal force redistribution due to steel plasticity, affecting the accuracy and reliability of the existing design provisions.

This paper describes assessments of the accuracy and reliability of the existing design provisions, namely SCI P355 [1], EN 1993-1-13 [23], and AISC DG31 [2], based on the results of extensive numerical simulations performed on cellular steel beams with span-to-depth ratios ranging from 15 to 30 and laterally restrained top flanges, reflecting the presence of the steel decking. The beams were loaded by a uniformly distributed load applied to the top flange, representing the most common condition encountered in the beam design. Although accuracy evaluations of the existing design provisions for non-composite cellular beams were published previously [25–27], the present authors are unaware of publications describing structural reliability evaluations of such beams. It should also be noted that [25,26] evaluated the accuracy of the SCI P355 [1] provisions only for the VBT failure mode, whereas [27] assessed the AISC DG31 [2] provisions only for LTB. Thus, prediction accuracy and reliability evaluations based on extensive numerical data presented in this paper are novel contributions. They highlight problematic areas that need to be resolved and provide directions on how improvements can be made.

The paper has the following structure. Section 2 provides an overview of the existing design provisions. Section 3 describes the numerical parametric study and the FE models of cellular beams. The performance of the existing design provisions compared with the FE results are presented in Section 4, followed by their reliability evaluation in Section 5. The results and future research directions are then discussed in Section 6.

2. Existing design provisions

The existing design provisions evaluated in this study, including SCI P355 [1], EN 1993-1-13 [23], and AISC DG31 [2], predict the cellular beam resistance from considering the BGS, BGB, VBT, WPS, WPB, and LTB failure modes. The LTB failure mode was eliminated through the provision of lateral restraints. The most significant differences between SCI P355 [1] and EN 1993-1-13 [23] on one side and AISC DG31 [2] on another consist in the former being based on the Eurocode framework [24,28], whilst the latter relied on the AISC 360 [29] provisions. The following subsections briefly describe the resistance calculations and the applicability limits in accordance with each design document.

The geometric beam parameters referred to in the present paper are given in Fig. 1. The design provisions for welded beams are discussed because such beams were studied in the present work.

2.1. SCI P355 [1]

The BGS resistance in SCI P355 is determined by comparing the design plastic shear resistance computed from Eq. (1) and the maximum vertical shear force at the opening center.

$$V_{\mathrm{pl,Rd}} = [t_{\mathrm{w}}(H - h_{\mathrm{o}})f_{\mathrm{y}}/\sqrt{3}]/\gamma_{\mathrm{M0}}, \tag{1}$$

where f_{y} is the steel yield strength and $\gamma_{\mathrm{M0}} = 1.00$ is the partial factor for resistance of cross-sections.

The BGB resistance is determined at the centers of the openings considering the cross-section classification of EN 1993-1-1 [24]. The BGB resistance is compared with the maximum internal moment at the opening centers due to the applied load.

The VBT resistance is determined by replacing circular openings with equivalent rectangular openings corresponding to a length, a_{eq}, of $0.45h_{\mathrm{o}}$ and a height, h_{eq}, of $0.90h_{\mathrm{o}}$. The VBT resistance is taken as the sum of the bending resistances of the Tees at four corners of the equivalent opening divided by the equivalent opening length (Eq. (2)). The VBT resistance computed from Eq. (2) is compared with the vertical shear force acting at the equivalent opening edge on the lower moment side.

$$V_{\mathrm{VBT,Rd}} = (2M_{\mathrm{bT,Rd}} + 2M_{\mathrm{tT,Rd}})/a_{\mathrm{eq}}, \tag{2}$$

where $M_{\mathrm{bT,Rd}}$ and $M_{\mathrm{tT,Rd}}$ are the design bending resistances of the bottom Tee and top Tee, respectively, reduced by the effects of the axial forces due to the global bending moment.

The WPS resistance, determined from Eq. (3), is checked against the horizontal shear force defined by Eq. (4).

$$V_{\mathrm{wp,Rd}} = (s_{\mathrm{o}}t_{\mathrm{w}}f_{\mathrm{y}}/\sqrt{3})/\gamma_{\mathrm{M0}} \tag{3}$$

$$V_{\mathrm{wp,Ed}} = sV_{\mathrm{Ed}}/h_{\mathrm{eff}}, \tag{4}$$

where V_{Ed} is the average of the design shear forces at the centers of the adjacent openings and h_{eff} is the effective beam depth measured between the centroids of the Tees.

The WPB resistance for closely spaced openings considered in this study is determined in accordance with EN 1993-1-1 [24] by assuming a buckling length of $l_{\mathrm{w}} = 0.5\sqrt{s_{\mathrm{o}}^2 + h_{\mathrm{o}}^2}$, with the non-dimensional slenderness expressed as $\bar{\lambda}_{\mathrm{wp}} = (1.75\sqrt{s_{\mathrm{o}}^2 + h_{\mathrm{o}}^2}/t_{\mathrm{w}})/\lambda_1$ (where λ_1 is the reference slenderness defined in EN 1993-1-1 [24]), and using EN 1993-1-1 [24] buckling curve c for welded beams. The WPB resistance is checked against the horizontal shear force defined by Eq. (4).

SCI P355 [1] requires the consideration of the effects of the high shear forces on the BGB and VBT resistances of cellular beams in accordance with EN 1993-1-1 [24]. The shear force is considered high when the ratio of the design shear force, V_{Ed}, at a section exceeds 50% of the design plastic shear resistance, $V_{\mathrm{pl,Rd}}$. The effects of the high shear forces can be accounted for by reducing the steel yield strength, f_{y}, or the beam web thickness, t_{w} by the factor $[1 - (2V_{\mathrm{Ed}}/V_{\mathrm{pl,Rd}} - 1)^2]$. In this study, the t_{w} reduction was used. It should be noted that this requirement did not affect the BGB resistance in this study because the shear forces were low near the beam mid-span, where the BGB resistance was determined.

SCI P355 [1] applies when the following geometric limits for the beams with circular openings are satisfied: $h_{\mathrm{o}} \le 0.8h$ (where $h = H + t_{\mathrm{f}}$); $h_{\mathrm{T}} \ge t_{\mathrm{f}} + 30$ mm (where $h_{\mathrm{T}} = (h - h_{\mathrm{o}})/2$); $s_{\mathrm{o}} \ge 0.3h_{\mathrm{o}}$; and $s_{\mathrm{e}} \ge 0.5h_{\mathrm{o}}$.

2.2. EN 1993-1-13 [23]

According to EN 1993-1-13 [23], the BGS resistance of welded beams is determined similarly to that in SCI P355 [1], except the plastic shear resistance of the perforated section should not exceed the shear buckling resistance of solid web computed per EN 1993-1-5 [28]. The BGB and WPS resistances according to EN 1993-1-13 [23] are computed using the same provisions as those in SCI P355 [1].

EN 1993-1-13 [23] offers two options for determining the VBT resistance of cellular beams. Option one is identical to the VBT resistance provisions in SCI P355 [1]. It is referred to as the 'main VBT provisions' in this paper. Option two is an alternative method that checks the interaction between the axial forces and bending moments determined on radial planes around each opening at angles from zero to $\phi_{\max} = \arctan(s/h)$, with the maximum acceptable angle increment of 5°. The second option is referred to as the 'alternative VBT provisions' in the present paper.

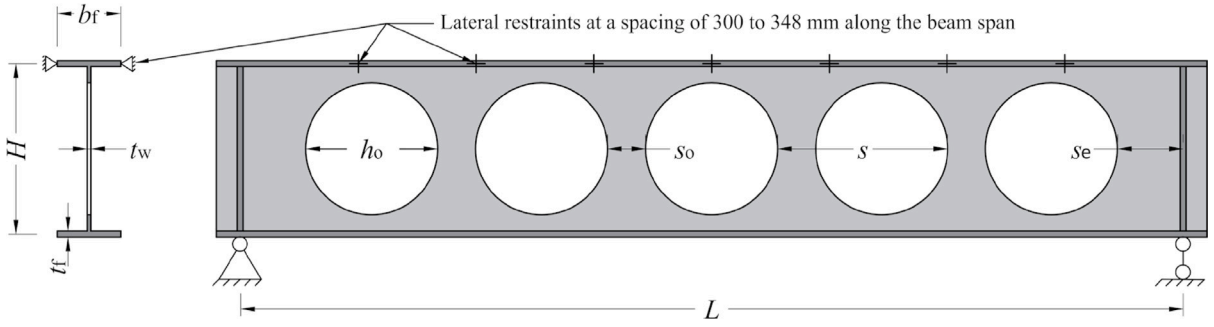

Fig. 1. Geometric parameters of cellular steel beams.

It was subsequently discovered by the present authors that when calculating the forces on the radial planes for the alternative VBT provisions, the magnitude of $V_{\phi,\mathrm{Ed}}$ could be high, resulting in the web of the top Tee sometimes being over-utilized in shear. In the absence of specific rules in EN 1993-1-13, the following equation was used to evaluate the shear forces on the inclined section [30]:

$$V_{\phi,\mathrm{Ed}} = \frac{A_{\mathrm{v},\phi}}{A_{\phi}} N_{\mathrm{m,Ed}} \sin(\phi) + V_{\mathrm{m,Ed}} \cos(\phi) - 0.5hw \sin(\phi), \tag{5}$$

where $A_{\mathrm{v},\phi}$ is the shear area of the inclined section, A_{ϕ} is the cross-sectional area of the inclined section, $N_{\mathrm{m,Ed}}$ and $V_{\mathrm{m,Ed}}$ is the design value of the axial force and shear force, respectively acting on the Tee at the middle of the opening due to global bending (i.e. $\phi = 0$), and w is the uniformly distributed load applied to the beam top flange. Eq. (5) ensures that only the axial force portion resisted by the web is considered to contribute to the shear force in the web.

The WPB resistance is calculated similarly to that in SCI P355 [1], except EN 1993-1-1 [24] buckling curve *a* is used (as opposed to buckling curve *c*). Also, the non-dimensional slenderness, $\bar{\lambda}_{\mathrm{wp}}$, cannot be taken greater than $(2.4h_{\mathrm{o}}/t_{\mathrm{w}})/\lambda_1$.

EN 1993-1-13 [23] includes the same provisions for considering the effects of the high shear forces on the BGB and VBT resistances as those in SCI P355 [1].

The EN 1993-1-13 [23] applicability limits are as follows: $h_{\mathrm{o}} \le 0.8h$; $h_{\mathrm{T}} \ge t_{\mathrm{f}} + 30$ mm; and $s_{\mathrm{o}} \ge 0.1h_{\mathrm{o}}$. When compared with SCI P355 [1], EN 1993-1-13 [23] permits narrower web-posts, s_{o}, and does not limit the end-post width, s_{e}, resulting in a much broader scope of application.

2.3. AISC DG31 [2]

AISC DG31 [2] references AISC 360 [29] for computing the BGS resistance as follows.

$$V_{\mathrm{n}} = 0.6 f_{\mathrm{y}} h t_{\mathrm{w}} C_{\mathrm{v1}}, \tag{6}$$

where C_{v1} is the web shear buckling coefficient determined by taking the web plate shear buckling coefficient, k_{v}, as 1.2 for the Tees.

The BGB resistance is computed at the opening centers in accordance with AISC 360 [29], considering the possibility of the local buckling of the flange or the stem in compression.

The VBT resistance calculations in AISC DG31 [2] are similar to those in SCI P355 [1] and EN 1993-1-13 [23] with the main VBT provisions, with the exception that the axial force and bending moment interaction checks are performed in accordance with AISC 360 [29].

The WPS resistance per AISC DG31 [2] is calculated similarly to that in SCI P355 [1] and EN 1993-1-13 [23].

The WPB resistance, computed as the web-post bending resistance determined with Eq. (7), is compared with the required flexural strength of the web-post calculated with Eq. (8) to determine if the beam WPB resistance is sufficient.

$$M_{\mathrm{n}} = [C1(s/h_{\mathrm{o}}) - C2(s/h_{\mathrm{o}})^2 - C3] t_{\mathrm{w}} (s - h_{\mathrm{o}} + 0.564h_{\mathrm{o}})^2 f_{\mathrm{y}}/6, \tag{7}$$

where $C1$, $C2$, and $C3$ are empirical coefficients determined as functions of $h_{\mathrm{o}}/t_{\mathrm{w}}$

$$M_{\mathrm{wp,Ed}} = 0.9(h_{\mathrm{o}}/2) V_{\mathrm{wp,Ed}} \tag{8}$$

Unlike SCI P355 [1] and EN 1993-1-13 [23], AISC DG31 [2] does not require f_{y} or t_{w} reductions due to high shear forces.

AISC DG31 [2] can be used under the following applicability limits: $1.25 \le h/h_{\mathrm{o}} \le 1.75$ and $1.08 \le s/h_{\mathrm{o}} \le 1.5$.

3. Numerical study

The data for evaluating the existing design provisions were obtained from FE simulations. The study considered simply-supported welded cellular I-beams, with the geometric parameters shown in Fig. 1. The lateral displacements of the beam top flanges were assumed to be restrained by a steel deck attached to the beam at a spacing ranging from 300 to 348 mm for different beams, representing the typical maximum flute spacing for modern steel deck profiles. The restraint spacing varied insignificantly for each beam due to the slightly different FE sizes used in different models predetermined by the web opening locations. The restraint spacing was kept constant for each beam. To cover cellular beams commonly used in construction, the following properties were varied:

- beam height between flange centers, H: 420, 560, and 700 mm;
- beam flange width, b_{f}: 162, 216, and 270 mm;
- beam web thickness, t_{w}: 9, 12, and 15 mm;
- beam flange thickness, t_{f}: 15, 20, and 25 mm;
- beam span-to-height ratio, L/H: 15, 20, 25, and 30;
- beam height-to-opening diameter ratio, H/h_{o}: 1.25, 1.50, and 1.70;
- opening spacing-to-opening diameter ratio, s/h_{o}: 1.10, 1.29, and 1.49;
- steel yield strength, f_{y}: 275, 355, and 460 MPa (which correspond to steel grades S275, S355, and S460, respectively).

The varied beam properties included span lengths found in real steel-framed buildings, the longer of which can only be achieved when the beams are restrained against the lateral–torsional buckling.

The web openings, with the centers located mid-height of the beam, were spread evenly along the beam span between the web stiffeners at the supports. For the cases where a web opening was not at mid-span (which corresponded to an even number of openings), additional models with an opening at mid-span were created by reducing the number of openings by one and re-arranging the opening locations, while keeping the opening spacing constant. Overall, 14,094 FE models were analyzed, with 8748 and 5346 models having an odd and even number of openings, respectively. The parameters of the modeled beams corresponded to all possible combinations of the varied properties listed above.

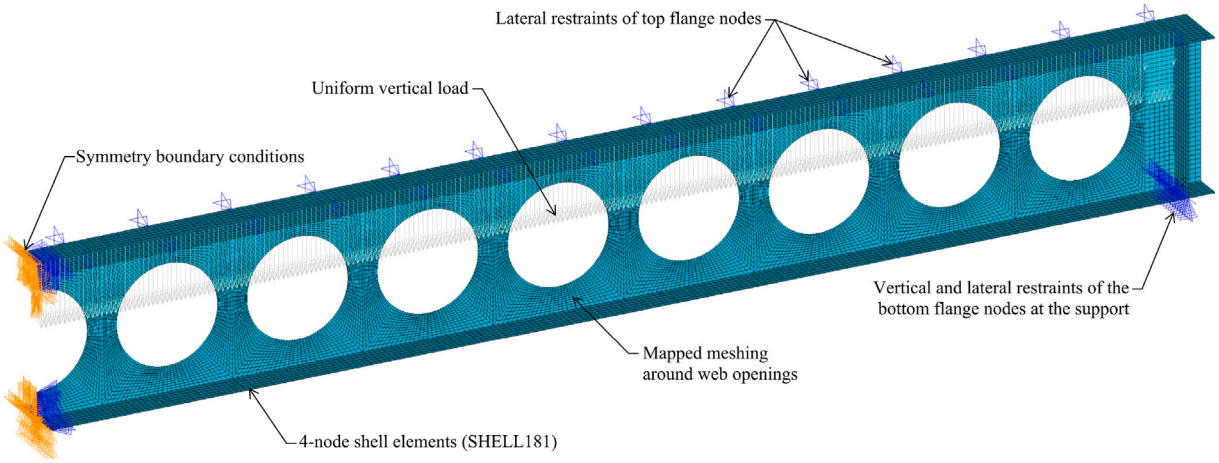

Fig. 2. Typical FE model used in the study.

3.1. FE models

In most studies describing FE simulations of cellular steel beams, the beams were modeled with shell elements [6–9,12–20]. In those models, the fillet radii between the beam flanges and the web or the fillet welds connecting the flanges to the web were not taken into account, which was compensated by the material overlap at the web-to-flange junctions [11]. Therefore, FE models of the cellular beams in this study were created in ANSYS using four-node shell elements with six degrees of freedom at each node, SHELL181. Full-height web stiffeners with a thickness equal to the beam flange thickness were assumed at the beam supports.

The models were meshed with quadrilateral elements with a maximum size of 20 mm. Mapped meshing with a spacing ratio of two was applied to the beam webs around the openings, resulting in the element sizes near the openings being two times smaller than the elements away from the openings. The appropriate mesh size was determined from a convergence study and confirmed by model validation results presented hereafter.

The material behavior of the steel was modeled with a bilinear stress–strain diagram without strain hardening (BISO) and von Mises yield criterion, which is one of the material models recommended by prEN 1993-1-14 [31] for hot-rolled steel. The modulus of elasticity and Poisson's ratio of steel were taken as 200 GPa and 0.3, respectively. Strain hardening was not considered in order to exclude the uncertainties associated with the yield plateau length and strain hardening modulus and to obtain more conservative FE simulation results. The consideration of strain hardening may produce higher capacities compared with the elastic-perfectly plastic diagram when the beam section or its parts reach the plastic stage [1]. The FE model validation results in sub- Section 3.2 confirm that the selected stress–strain diagram was appropriate.

The boundary conditions of the models presented in Fig. 2 were introduced to simulate simply-supported beams. Explicit simulations of fork supports commonly used in previous studies [6,8,16,18] were not required because the periodic lateral restraints of the top flange (which started and ended near the supports) did not allow the beam top flange to move laterally, whereas the bottom flange nodes were laterally restrained at the supports (see Fig. 2). In other words, the boundary conditions of the modeled beams at the supports were similar to those provided by fork supports. Due to symmetry, one-half of the beam was modeled, and symmetry boundary conditions were applied at the beam mid-span. Vertical forces with magnitudes proportional to the element size were applied to the beam top flange at the web location, simulating a uniformly distributed load, which is most commonly used in the design of steel beams.

Initial geometric imperfections and residual stresses were considered in the models. The initial geometric imperfection shape corresponded to the first buckling mode of the beams obtained from the elastic buckling analyses, which preceded the nonlinear static analyses. The magnitude of the imperfections were taken as $H/100$ for $L/H < 10$ and $L/1000$ for $L/H \geq 10$ [11,18,20].

The residual stresses followed the recommendations given in [11,16,32]: compressive residual stresses at the flange edges were 100 MPa for $(H + t_f)/b_f > 1.2$ and 150 MPa for $(H + t_f)/b_f \leq 1.2$; tensile residual stresses at the flange center were 50 MPa for $(H + t_f)/b_f > 1.2$ and 100 MPa for $(H + t_f)/b_f \leq 1.2$; and tensile residual stresses in the web were $50 b_f t_f/((H - h_o)t_w)$. It should be noted that experimental data on the residual stresses in cellular steel beams is limited. The only experimental investigation on this topic known to the authors is presented in [11,32], where the residual stresses were measured in cellular steel beams of grade S275 fabricated from hot-rolled parent sections cut longitudinally, after which the beam halves were shifted and welded. While several residual stress distribution models have been proposed for welded beams with solid webs [33–36], such models do not exist for welded cellular steel beams and beams of steel grades other than S275. Therefore, the residual stress distribution proposed in [11,16,32] was assumed to apply to the studied beams fabricated similarly to those in [11,32]. The same approach was taken in [12]. It is worth noting that a comparative analysis of the effect of the residual stress distributions on the FE model predictions presented in [37] demonstrated that the ultimate loads for the Sonck model [11,16,32] differed from the models for welded solid-web beams [33,34,36] by −1 to 10%, with an average difference of 3% for four considered composite cellular beams, implying a relatively small effect of the residual stress distribution model on the FE model predictions.

The nonlinear static analysis accounted for the geometric and material nonlinearities. The beam resistance was taken as the minimum of the maximum load the model could support (criterion C1 in prEN 1993-1-14 [31]) and the load corresponding to the largest tolerable strain (criterion C2 in prEN 1993-1-14 [31]). The largest tolerable total strains were taken as 23%, 22%, and 17% for steel grades S275, S355, and S460, respectively, in accordance with EN 10025-2 [38]. These values were considered more realistic for the studied beams than the maximum acceptable plastic strain of 5% given in EN 1993-1-5 [28]. The largest tolerable strain was compared with the maximum strain from the integration (Gauss) points of the shell elements.

3.2. FE model validation

The FE models were validated against ten test results described in [3,4,7,8]. The only differences between the FE models used in the

Table 1
FE model validation results.

No.	Source	Test	H (mm)	b_f (mm)	t_w (mm)	t_f (mm)	L/H	H/h_o	s/h_o	f_y (MPa)	FM	P_{test} (kN)	P_{FEA} (kN)	P_{test}/P_{FEA}
1	[3]	1B	282	133	5.8	7.8	20	1.41	1.50	323	VBT	108.0	109.5	0.99
2	[3]	2B	302	133	5.8	7.8	19	1.34	1.33	343	VBT	117.0	119.6	0.98
3	[3]	3A	428	102	5.8	6.8	9	1.43	1.50	350	VBT	151.0	151.4	1.00
4	[3]	4A	456	102	5.8	6.8	18	1.40	1.23	437	BGB	90.0	90.0	1.00
5	[3]	4B	456	102	5.8	6.8	16	1.40	1.23	360	WPB	114.0	118.2	0.96
6	[7]	A1	439	152	7.6	10.9	4	1.39	1.30	360	WPB	288.7	286.8	1.01
7	[7]	B1	439	152	7.6	10.9	4	1.39	1.20	360	WPB	255.0	247.0	1.03
8	[4]	1-ss	544	180	8.6	13.6	3	1.52	1.34	338	WPB	500.0	490.9	1.02
9	[8]	A1	426	104	4.7	5.5	4	1.23	1.14	415	WPB	76.0	78.8	0.96
10	[8]	B6	400	98	6.0	9.2	4	1.63	1.40	390	WPB	299.9	304.2	0.99

validation compared with the parametric numerical study were the beam geometry and load application (concentrated loads in the model validation vs. uniform loads in the numerical study).

The tests were selected to ensure that the parameters of the tested beams were close to those in the study, and various failure modes were represented. The parameters of the selected beams and FE model validation results are summarized in Table 1.

It should be noted that the geometric parameters of the tested beams were smaller than those used in the study because smaller specimens are preferred in experimental studies, while the presented work aims to study the beam sizes commonly used in construction. However, the ranges of the relative dimensions in the tests, L/H, H/h_o, s/h_o, and f_y were close to those considered within the study.

Table 1 shows that the selected tests covered different failure modes, including VBT, BGB, and WPB. The authors could not find test results for the BGS and WPS suitable for FE model validation, while the tests failing in LTB were excluded because this failure mode was beyond the scope of the study.

As can be seen from Table 1, the test-to-prediction ratios, P_{test}/P_{FEA}, ranged from 0.96 to 1.03, with a mean value of 0.99 and a coefficient of variation (CoV) of 0.022, indicating a good prediction accuracy of the FE models. Additionally, comparisons of the load–displacement curves presented in Fig. 3 demonstrate a good agreement between the experimental and numerical data throughout the entire range of loading. It can be concluded that the developed FE models could accurately predict the behavior and resistance of actual beams. Therefore, they were appropriate for the FE numerical study described in the next sub-section.

3.3. Numerical study results

The numerical study results are summarized in Fig. 4, which presents the effects of the studied parameters on the ratio of the ultimate moment, M_u, to the plastic moment, M_{pl}, at the beam mid-span. Each graph shows violin plots representing M_u/M_{pl} distributions and line plots of the mean M_u/M_{pl} values for each parameter value.

Fig. 4(a) indicates that the M_u/M_{pl} values ranged from 0.13 to 1.00 for all considered beam heights. The average M_u/M_{pl} values were practically the same for the studied H values: 0.69, 0.71, and 0.71 for 420, 560, and 700-mm deep beams, respectively.

The M_u/M_{pl} values increased when t_w increased, as presented in Fig. 4(b). The M_u/M_{pl} ranges were 0.13 to 1.00, 0.19 to 1.00, and 0.23 to 1.00 for web thicknesses of 9, 12, and 15 mm, respectively (with average values of 0.63, 0.72, and 0.76). These results can be explained by a higher sensitivity of beams with thinner webs to web buckling failure modes when compared to similar beams with thicker webs, which resulted in lower plastic resistance moment utilization for the beams with smaller t_w values.

According to Fig. 4(c) and (d), M_u/M_{pl} decreased when t_f and b_f increased, which was driven by the beams failing in web-related failure modes before reaching the plastic moment resistance, which was greater for the beams with larger flanges. The M_u/M_{pl} values ranged from 0.20 to 1.00, 0.16 to 1.00, and 0.13 to 1.00 for flange thicknesses of 15, 20, and 25 mm, respectively (with average values of 0.74, 0.70, and 0.67). For b_f of 162, 216, and 270 mm, M_u/M_{pl} ranged from 0.18 to 1.00, 0.15 to 1.00, and 0.13 to 1.00 (with average values of 0.75, 0.71, and 0.66), respectively.

Fig. 4(e) presents the effect of H/h_o on M_u/M_{pl}. It can be seen that M_u/M_{pl} increased when H/h_o increased, indicating the positive effect of the relative opening size reduction on the plastic moment capacity utilization. For H/h_o of 1.25, 1.50, and 1.70, M_u/M_{pl} ranged from 0.13 to 1.00, 0.15 to 1.00, and 0.17 to 1.00 (with average values of 0.66, 0.71, and 0.74), respectively.

The s/h_o ratio had the most significant effect on M_u/M_{pl} among the studied parameters, as Fig. 4(f) shows. M_u/M_{pl} increased from 0.40 to 0.85 on average when s/h_o increased from 1.10 to 1.29, with a further average increase from 0.85 to 0.89 when s/h_o changed from 1.29 to 1.49. For s/h_o of 1.10, 1.29, and 1.49, the M_u/M_{pl} ranges were from 0.13 to 1.00, 0.30 to 1.00, and 0.41 to 1.00, respectively. The M_u/M_{pl} distributions for s/h_o = 1.10 differ significantly from those for s/h_o of 1.29 and 1.49. Most M_u/M_{pl} values for s/h_o = 1.10 concentrated around 0.40, and only a few beams reached the plastic moment capacity, whereas the wider opening spacings produced a fuller plastic moment capacity utilization, with many beams reaching the plastic moment capacity. These results indicate that the relative opening spacing, s/h_o, is the most significant parameter affecting the cellular beam resistance.

Fig. 4(g) demonstrates that M_u/M_{pl} increased when L/H increased. The most significant gain in M_u/M_{pl}, from 0.63 to 0.71 on average, occurred when L/H increased from 15 to 20. The further increase in L/H up to 30 resulted in smaller M_u/M_{pl} rises, characterized by average M_u/M_{pl} values of 0.72 and 0.74 for L/H of 25 and 30, respectively. For L/H of 15, 20, 25, and 30, the M_u/M_{pl} ranges were 0.13 to 1.00, 0.16 to 1.00, 0.18 to 1.00, and 0.20 to 1.00, respectively. These results indicate that longer spans allow for a better redistribution of the beam internal forces and a fuller plastic moment capacity utilization than shorter spans.

All graphs in Fig. 4 indicate that the M_u/M_{pl} values decreased when f_y increased, which aligns well with the structural steel design principles. Higher yield stresses make steel beams more susceptible to buckling failure modes before reaching the plastic moment resistance, which is proportional to f_y.

The von Mises stress contour plots on deformed beam shapes at failure illustrate multiple interactions of various failure modes. Fig. 5 shows several examples of the plots. It can be seen that the beam in Fig. 5(a) showed the signs of the VBT, WPB, and WPS failure modes, while the beam in Fig. 5(b) failed in VBT, WPS, BGB, and perhaps BGS. The beam in Fig. 5(c) failed in BGB, with the elastic buckling of the wide web-posts near the beam support clearly noticeable. The beam in Fig. 5(d) exhibited VBT and WPS failure modes, while the beam in Fig. 5(e) failed in BGB, WPS, and perhaps BGS.

Due to the multiple failure mode interactions, it was found challenging, if not impossible, to reliably determine primary failure modes for all models from the images. The FE simulation results obtained in the study were compiled within a database available in [39]. The database includes images of the von Mises stress contour plots at the beam failures, which may be used for identifying failure modes for each beam.

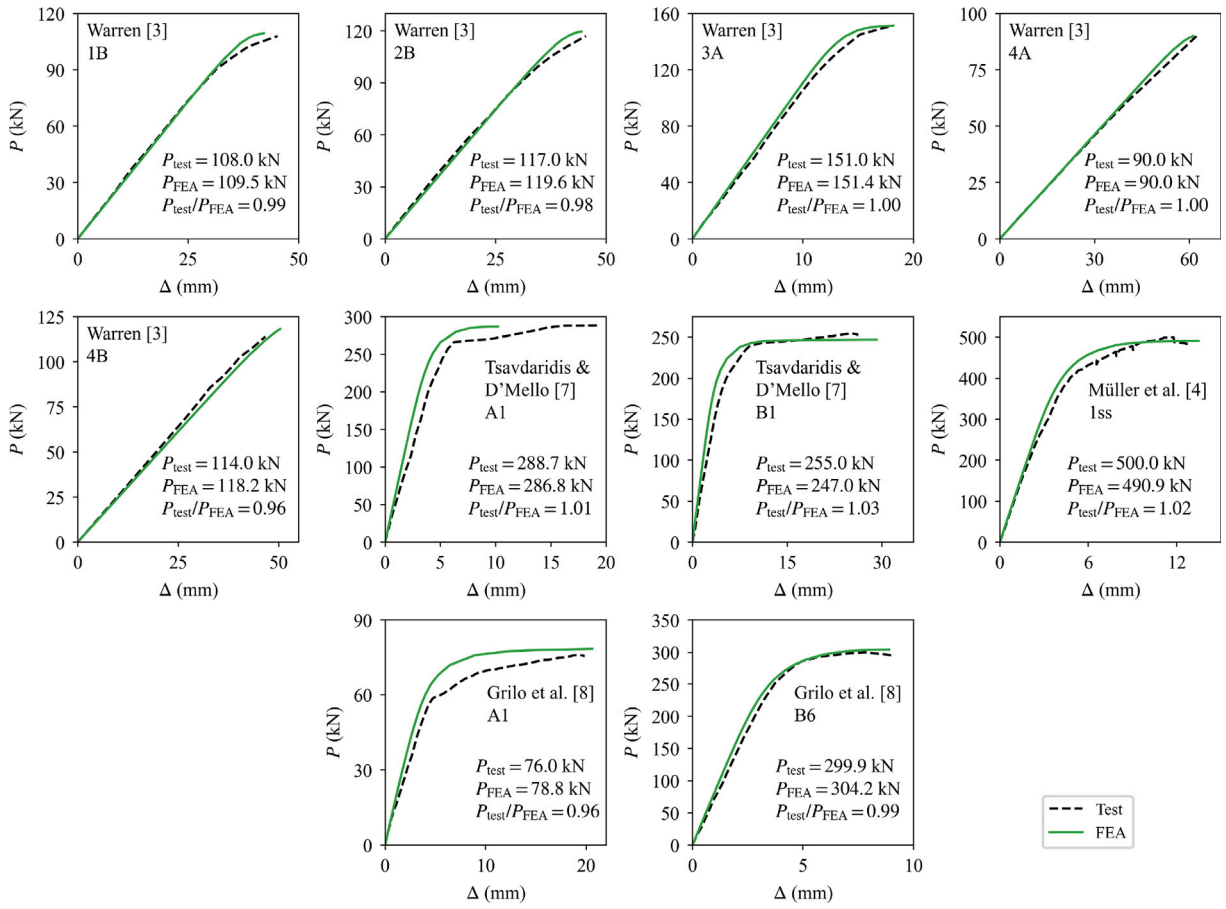

Fig. 3. Comparisons of the load–displacement curves from the tests and FE simulations.

4. Accuracy assessments

This section describes accuracy assessments of the existing design provisions in predicting the resistance of laterally restrained cellular beams by comparing the FE simulation results with the predictions from the design provisions. The applicability limits, which vary in each provision (see Section 2), were considered in the comparisons, resulting in different numbers of beams, n, used in the comparisons with the different design documents. The comparisons were made in terms of the coefficient of determination ($R^2 = 1 - \sum_{i=1}^{n}(y-x)^2 / \sum_{i=1}^{n}(y-\bar{y})^2$, where n is the number of observations, y is the observed values, and x is the predicted values, and $\bar{y}$ is the mean value of y), which was shown to be more informative than other performance metrics in [40], together with the mean and the CoV of the simulation-to-prediction ratios, referred to as the resistance ratios (RRs) throughout this paper.

The uniform loads for the existing design provisions were obtained from the calculated beam resistances for each failure mode and the corresponding moment or shear diagrams for a simply-supported beam. A direct calculation of the uniform load, w, governed by the VBT resistance of beams with the web thickness reduction due to high shear was impossible. Therefore, the following iterative procedure was used: (1) the uniform load for unreduced t_w was assumed; (2) the beam web thickness was reduced based on the applied shear forces due to w where needed; (3) the Eurocode M and N interaction equation was checked; (4) if the interaction equation was satisfied, the w value assumed in step 1 was taken as w for the beams with the reduced t_w; and (5) otherwise, w was reduced and steps 2 to 4 were repeated until the interaction equation was satisfied. The minimum uniform load for all failure modes was taken as the ultimate load value. The failure mode corresponding to the ultimate load was taken as the primary failure mode of the beam predicted by the design documents. The comparisons were made for all evaluated steel grades and failure modes combined and separately.

Detailed calculation examples for each considered design method can be found in [39]. The interactive example files, developed in SMath Studio (https://smath.com/), a free mathematical notebook program, allow for generating calculations for any beam from the database [39]. The database includes the ultimate uniform loads computed in accordance with the considered design methods for each simulated beam in addition to the FE simulation results.

4.1. Comparisons of the FE simulation results with the design provision predictions

Fig. 6 compares uniform ultimate loads predicted by SCI P355 [1] with those obtained from the FE simulations. For 2997 beams complying with the applicability limits, SCI P355 [1] predicted the BGS, BGB, VBT, WPS, and WPB failure modes for 492 (16.4%), 1780 (59.4%), 567 (18.9%), 111 (3.7%), and 47 (1.6%) beams, respectively.

For all considered steel grades and failure modes, the mean and CoV values of the RRs were 1.13 and 0.185, respectively, which indicates reasonable accuracy of the SCI P355 [1] provisions. The mean RRs and their scatter increased when the steel grade increased.

The largest RR scatters were obtained for the BGS and VBT failure modes, ranging from 0.157 to 0.162 for BGS and from 0.109 to 0.247 for VBT. The mean and CoV values of the BGS RRs practically did not change when the steel grade varied. For VBT, the mean and CoV values of the RRs increased significantly (from 1.16 to 1.32 and 0.109 to 0.247, respectively) when the steel grade increased from S275 to S355. The steel grade change from S355 to S460 resulted in a slight increase in the mean RR from 1.32 to 1.35 and a reduction in the CoV

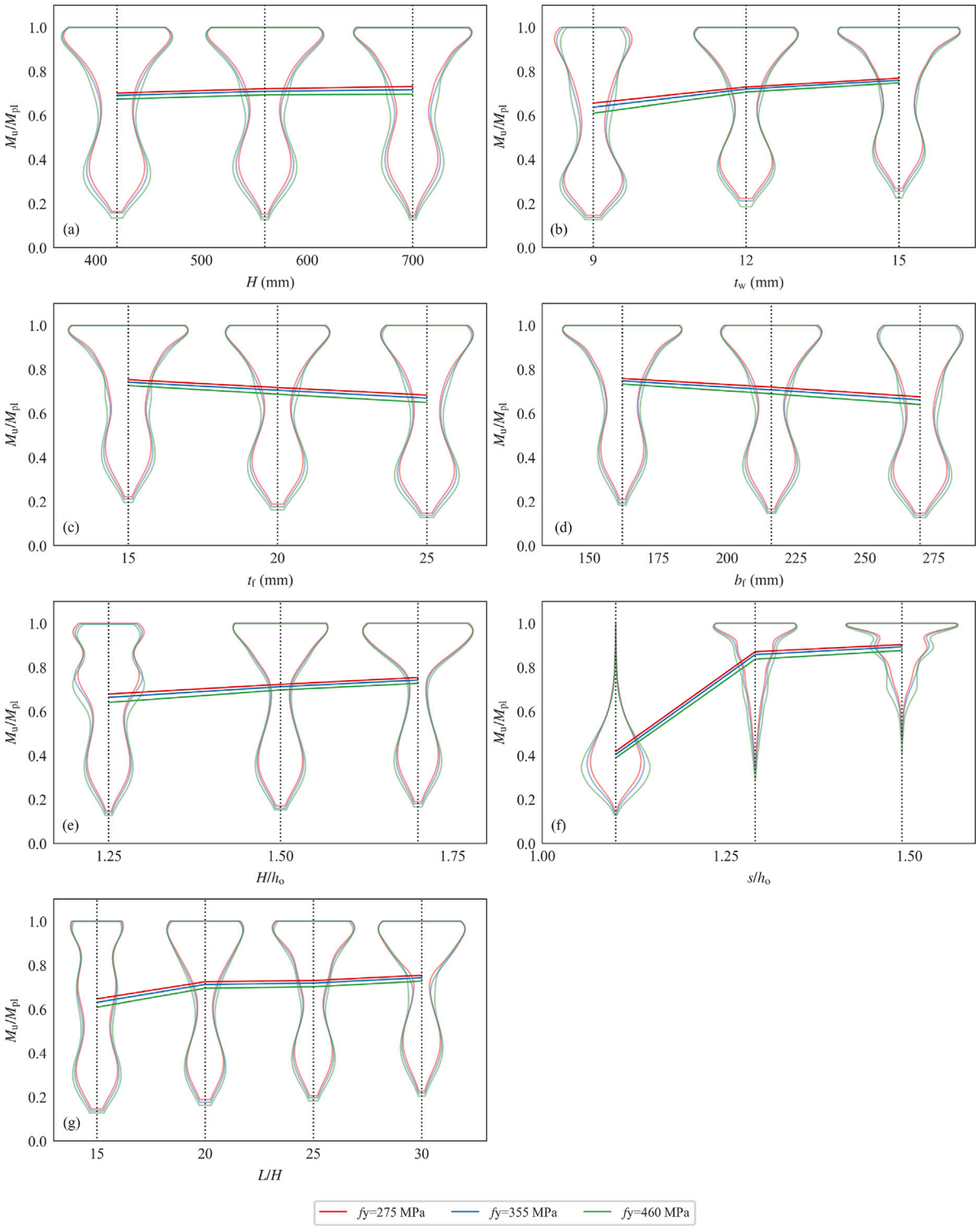

Fig. 4. Effects of the studied parameters on M_u/M_{pl} at the beam mid-span.

from 0.247 to 0.226. It should be noted that the observed dependence of the VBT RRs from the steel grade may be caused by the significantly different numbers of samples representing various steel grades (68, 222, and 277 for S275, S355, and S460, respectively).

The predictions for the BGB, WPS, and WPB failure modes showed considerably better agreements with the simulation results than those for BGS and VBT, especially for BGB, characterized by a mean RR value of 1.02 for all steel grades, with coefficients of variations increasing from 0.032 to 0.055 when the steel grade increased. The mean and CoV values for WPS decreased from 1.19 to 1.17 and from 0.072 to 0.055, respectively, when the steel grade increased. The dependence of the WPB RRs on the steel grade observed from Fig. 6 can be misleading due to the significantly different number of samples representing each steel grade.

Fig. 7 presents comparisons of the EN 1993-1-13 [23] predictions when the main VBT provisions were considered with the FE simulation

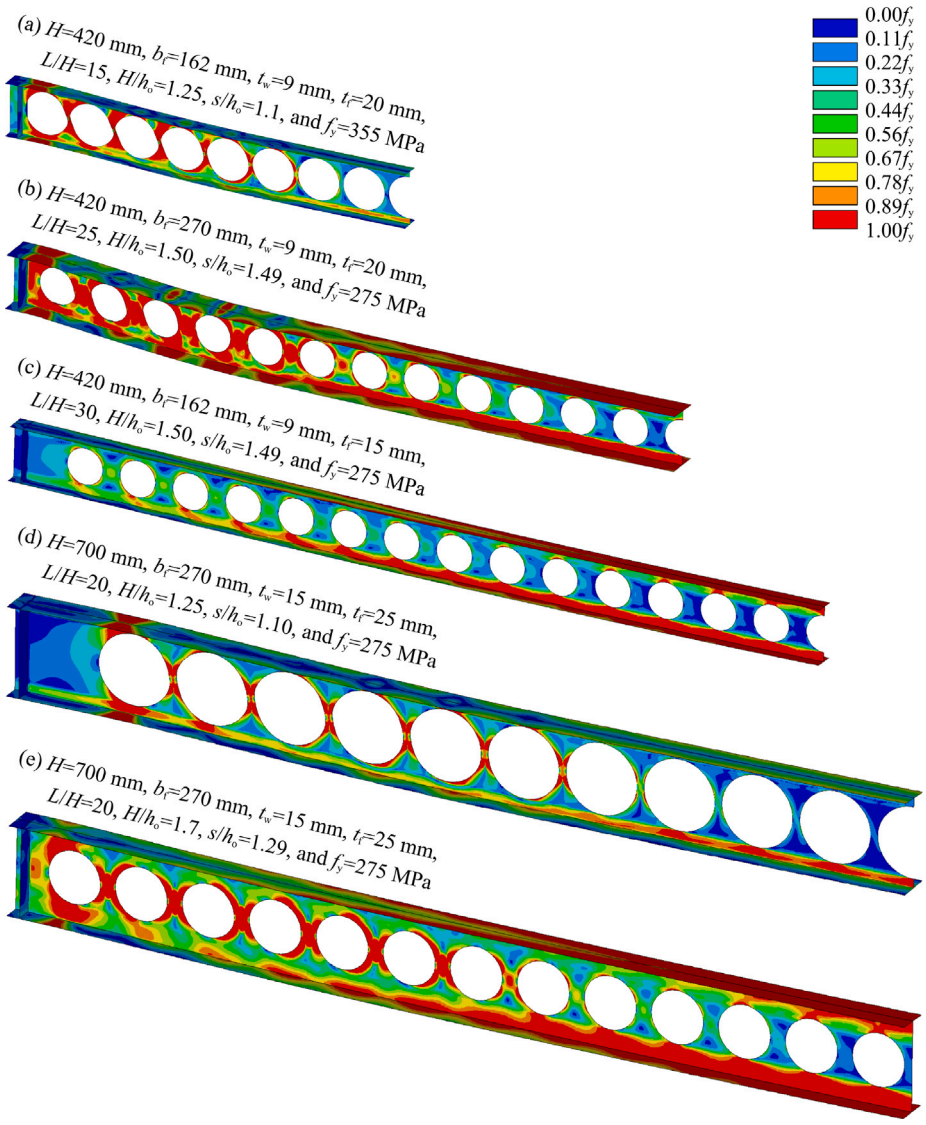

Fig. 5. Examples of von Mises stress contours at the failure.

results. Due to the broader applicability limits of EN 1993-1-13 [23] compared with SCI P355 [1] (see Section 2) significantly more beams were included in the EN 1993-1-13 [23] comparisons than for SCI P355 [1] (13,554 vs. 2997). The Eurocode predicted the BGS, BGB, VBT, WPS, and WPB failure modes for 1004 (7.4%), 4647 (34.3%), 1415 (10.4%), 5711 (42.1%), and 777 (5.7%) beams, respectively. The percentage of the beams failing in WPS and WPB according to EN 1993-1-13 [23] significantly increased compared with SCI P355 [1], while the percentages of the BGS, BGB, and VBT failure modes decreased. This can be explained by the narrower web-posts permitted by EN 1993-1-13 [23], which were susceptible to WPS and WPB failures.

The accuracy of the EN 1993-1-13 [23] predictions is similar to that of SCI P355 [1]. The Eurocode demonstrated excellent accuracy in predicting the BGB and WPB resistances and reasonable accuracy in the BGS, VBT, and WPS resistance predictions. Because EN 1993-1-13 [23] and SCI P355 [1] specify similar calculation methods for the BGS, BGB, VBT, and WPS resistances, the differences in the accuracy metrics between the two design documents can be explained by the broader scope of EN 1993-1-13 [23], resulting in the larger number of the considered cases.

The WPB resistance predicted by EN 1993-1-13 [23] was closer to the simulation results than the SCI P355 [1] predictions, with the mean RR value for all analyzed steel grades of 1.02 vs. 1.22 for SCI P355 [1]. The difference can be explained by the smaller imperfection factor specified in EN 1993-1-13 [23] (0.21 for buckling curve *a*) than that in SCI P355 [1] (0.49 for buckling curve *c*). However, the RR scatters are larger for EN 1993-1-13 [23] than those for SCI P355 [1] (0.118 vs. 0.054), which can be explained by the larger number of beams within the EN 1993-1-13 [23] scope.

Fig. 8 compares the beam resistances computed following EN 1993-1-13 [23] with the alternative VBT provisions. The Eurocode predicted the BGS, BGB, VBT, WPS, and WPB failure modes for 37 (0.3%), 1001 (7.4%), 6291 (46.4%), 5529 (40.8%), and 696 (5.1%) beams, respectively. The percentage of the beams failing in VBT significantly increased for the alternative provisions compared with the main provisions, indicating that the former produces lower VBT resistances than the latter.

Fig. 8 also shows that the mean RR values and their CoVs for the VBT failure mode according to the alternative provisions were smaller than those using the main provisions (1.17 vs. 1.25 and 0.175 vs.

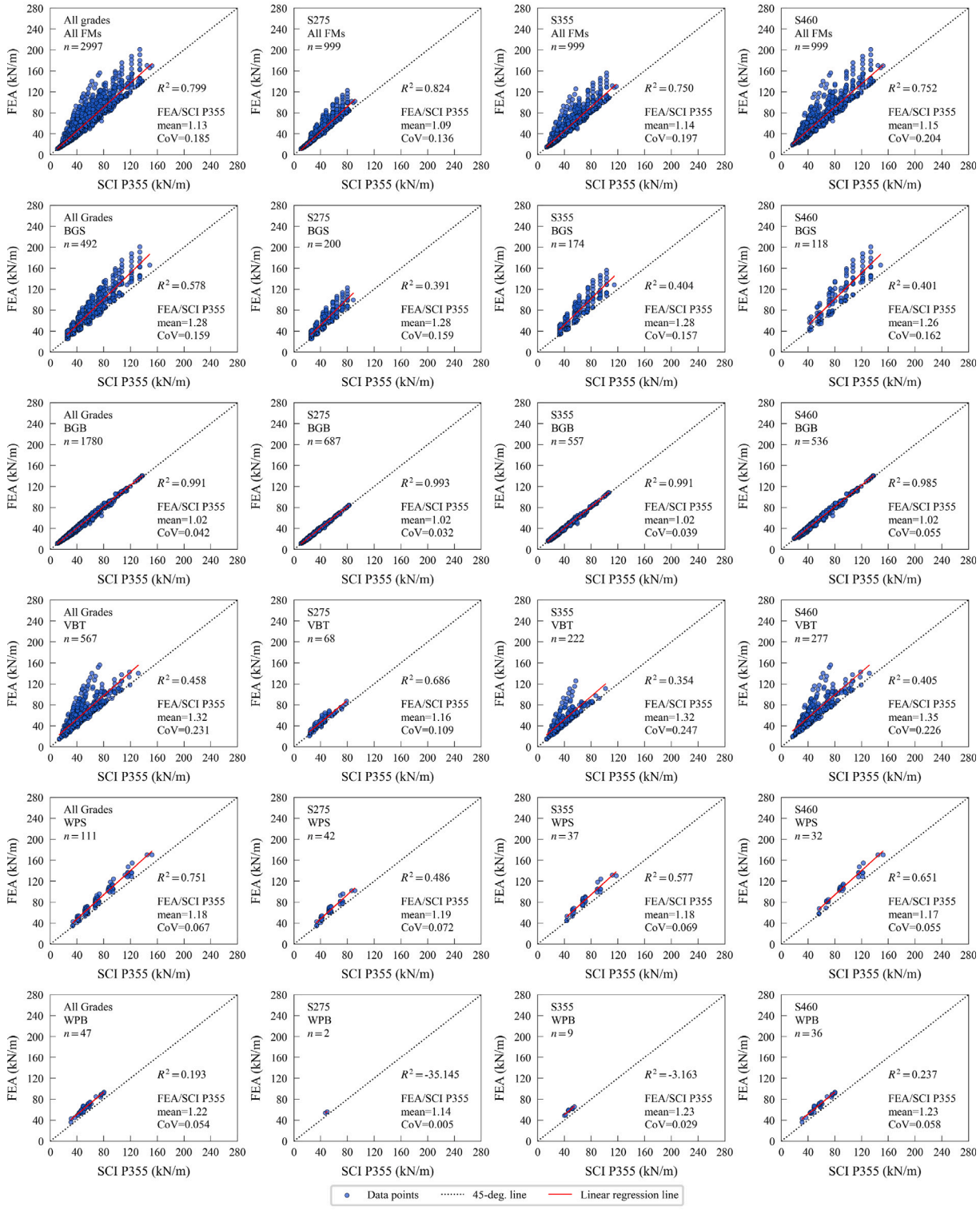

Fig. 6. Comparisons of the FE simulation results with the SCI P355 [1] predictions.

0.204 for all steel grades). The prediction accuracy of EN 1993-1-13 [23] with the alternative VBT provisions for the BGB, WPS, and WPB failure modes was comparable with this Eurocode when the main VBT provisions were used. For BGS, the alternative VBT method resulted in higher RR means (1.45 vs. 1.20) and lower RR CoVs (0.112 vs. 0.143) due to significantly different numbers of beams failing in BGS (37 and 1004 for the alternative and main method, respectively), considering that the same BGS provisions were used in both cases.

The AISC DG31 [2] predictions are compared with the FE simulation results in Fig. 9. Out of 10,854 beams within the design guide applicability limits, 5833 (53.7%) and 5021 (46.3%) failed in the VBT and WPB, respectively, according to the design guide. No other failure modes were predicted.

The accuracy metrics in Fig. 9 demonstrate a worse prediction accuracy for AISC DG31 [2] compared with SCI P355 [1] and EN 1993-1-13 [23], characterized by larger mean and CoV values of the RRs. The

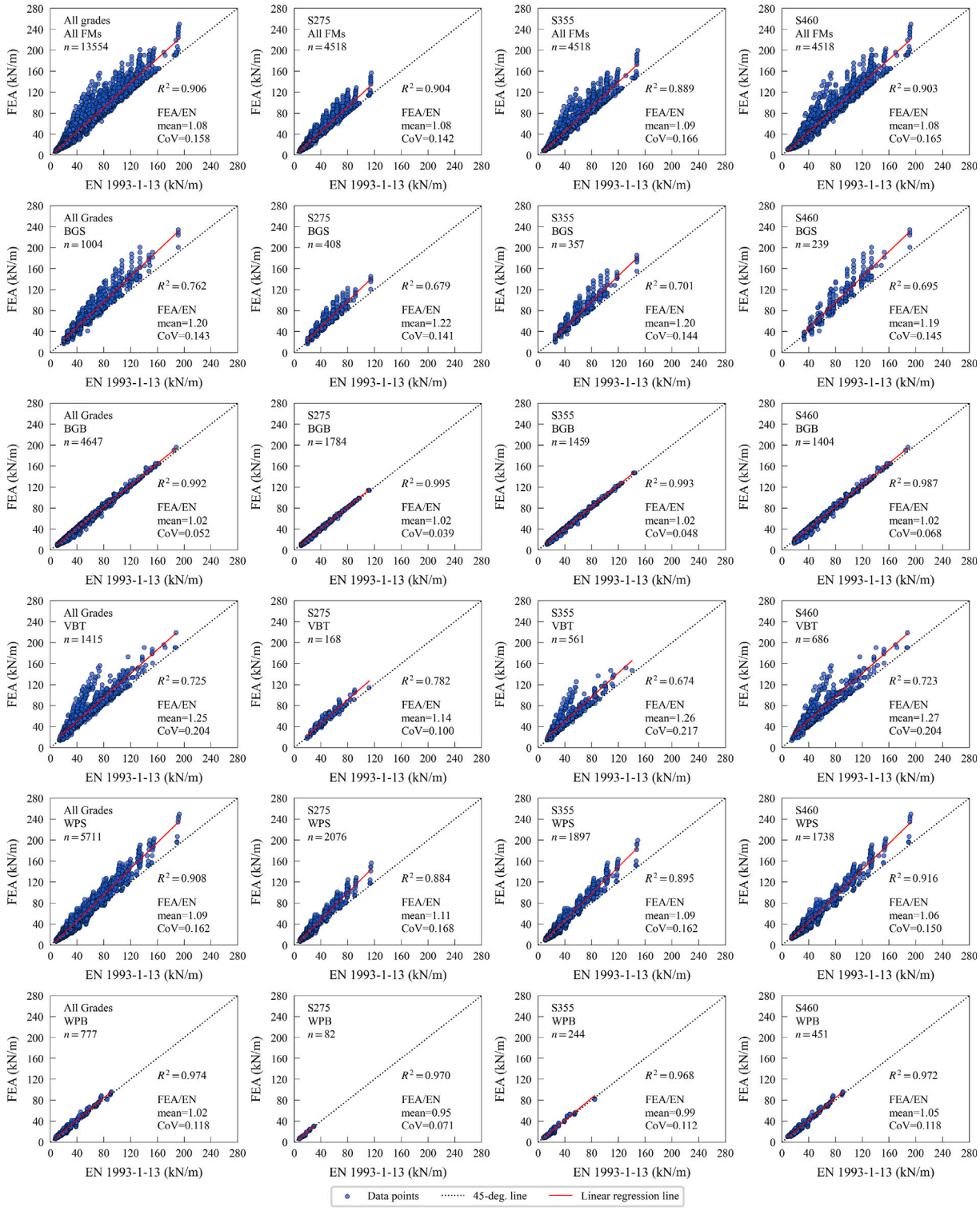

Fig. 7. Comparisons of the FE simulation results with the EN 1993-1-13 [23] predictions (the main VBT provisions).

RR means and CoVs decreased when the steel grade increased for the VBT and WPB failure modes predicted by AISC DG31 [2].

4.2. Effects of beam parameters on the resistance prediction accuracy

According to Figs. 6–8, the existing design provisions resulted in larger RR scatters for the VBT, WPS, and BGS failure modes than those for BGB and WPB. Therefore, the effects of the cellular beam parameters on the accuracy predictions for the VBT, WPS, and BGS resistances were analyzed to discover potential directions for improving the prediction accuracy.

It was found that H/h_o affected the RRs for the VBT failure mode more than other variables, as Fig. 10 shows. The blue dots in the figure represent data points, whilst the red lines connect the RR mean values for each H/h_o value. The green lines show the violin plots of the RR distributions, illustrating the scatter.

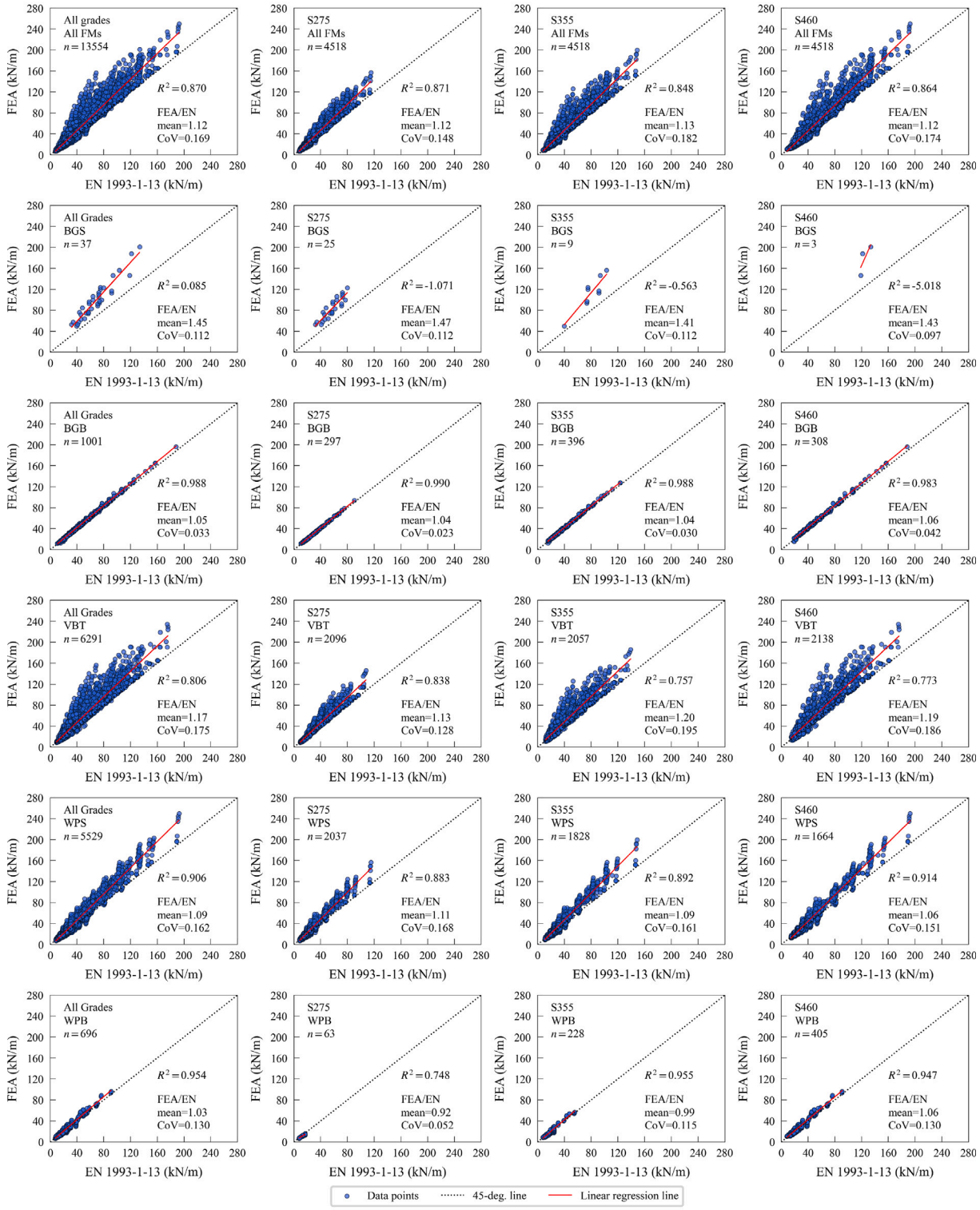

Fig. 8. Comparisons of the FE simulation results with the EN 1993-1-13 [23] predictions (the alternative VBT provisions).

Fig. 10 indicates that the mean values and the scatter of the RRs for all considered design provisions increased when H/h_o decreased, especially from 1.50 to 1.25. These results indicate that the design provisions perform worse in predicting the VBT resistance for cellular beams with relatively shallow Tees when compared to the beams with deeper Tees. SCI P355 [1], the main VBT method of EN 1993-1-13 [23], and AISC DG31 [2], which employ the equivalent opening approach, demonstrated greater increases in the RRs when H/h_o decreased from 1.50 to 1.25 than the alternative VBT method of EN 1993-1-13 [23]. These results indicate that the prediction accuracy of the existing design

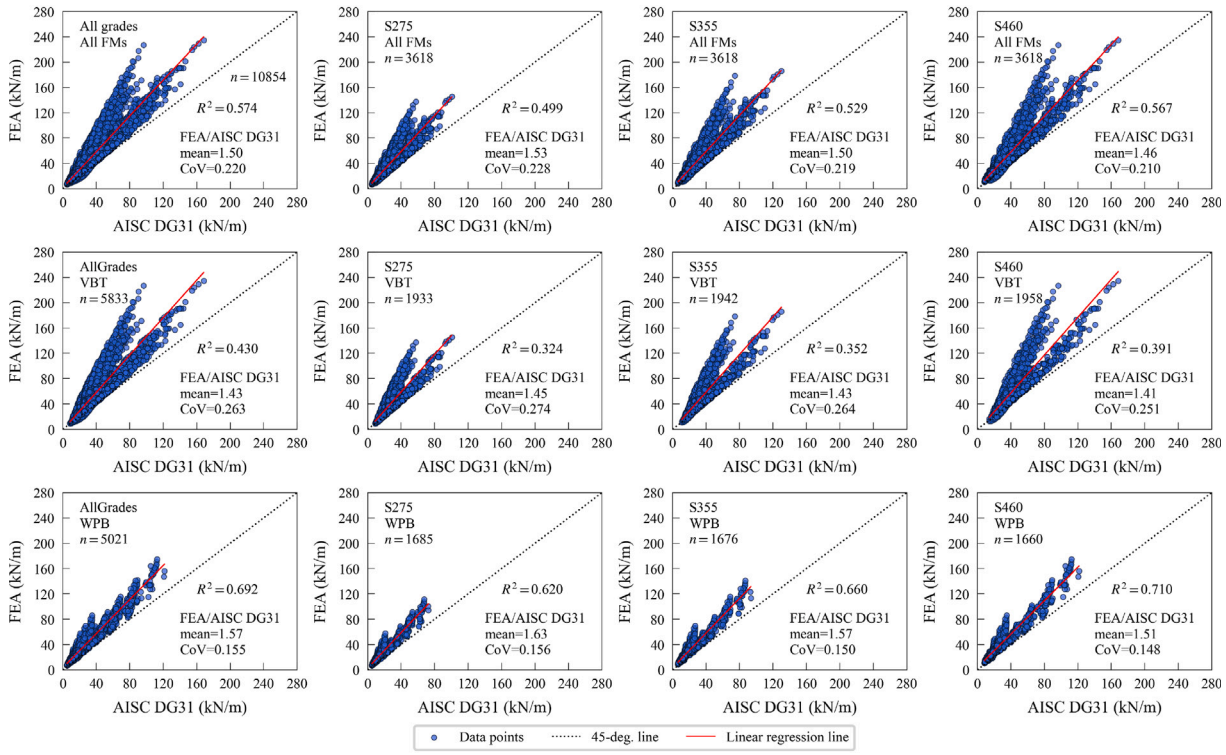

Fig. 9. Comparisons of the FE simulation results with the AISC DG31 [2] predictions.

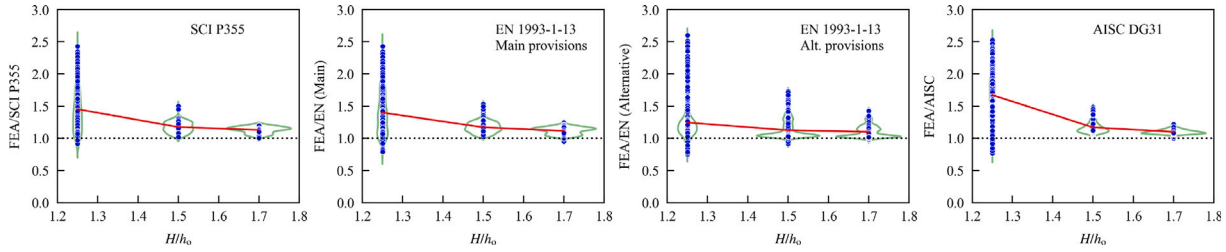

Fig. 10. Effects of H/h_o on the prediction accuracy for the VBT resistance of cellular beams.

provisions can be improved by refining the equivalent opening size determination which, as opposed to the current linear relationship (see Section 2), may depend on a nonlinear relationship with h_o.

It was also found that the RRs for the WPS beam resistance predicted by the existing provisions depends on h_o, as illustrated in Fig. 11. The RRs increased when the opening size decreased, implying that an equivalent opening approach, with the equivalent opening size depending on h_o, may be appropriate for the WPS resistance calculations, which would be equivalent to allowing the horizontal shear stress to exceed $f_y/\sqrt{3}$ at the web-post center.

Fig. 12 indicates that the BGS RRs depend on the ratio of the web area at the opening center (A_w) to the flange area (A_f) and L/H. The former highlights the flange contribution to the BGS resistance, especially in the beams with shallow Tess represented by low A_w/A_f ratios. The dependence of the BGS RRs on L/H implies that the moment gradient may affect the BGS resistance of cellular beams. Therefore, considering the flange contribution to the BGS resistance and the moment gradient may improve the BGS resistance predictions of the existing design provisions.

5. Reliability assessments

The reliability of the existing design provisions was assessed using two approaches. The first approach consisted of partial factor determination in accordance with EN 1990 [44] Annex D for both SCI P355 [1] and EN 1993-1-13 [23], and load and resistance factor design (LRFD) resistance factor and allowable strength design (ASD) safety factor calculations in accordance with AISI S100 [45] Chapter K after appropriate modifications for AISC DG31 [2]. The second approach used the improved Hasofer–Lind–Rackwitz–Fiessler (iHL–RF) method [46–48], which is a variation of the first-order, second-moment reliability method.

5.1. Partial factors for SCI P355 [1] and EN 1993-1-13 [23] in accordance with EN 1990 [44] Annex D

Partial factors required for the resistance against each failure mode predicted by SCI P355 [1] and EN 1993-1-13 [23] were determined in accordance with EN 1990 [44] Annex D, by treating the FE simulation results as experimental resistance values, r_e, and the design provision predictions as theoretical resistance values, r_t.

The FE simulation results were not modified by an FE model factor as suggested, for example, by prEN 1993-1-14 [31] because a study of the FE model factor values determined using different methods performed as a part of this work demonstrated that the FE model factor might be overly conservative. The present paper does not discuss the FE model factor study results further due to space limitations. The authors believe more research on this topic is needed to justify an appropriate procedure for computing the FE model factor that does

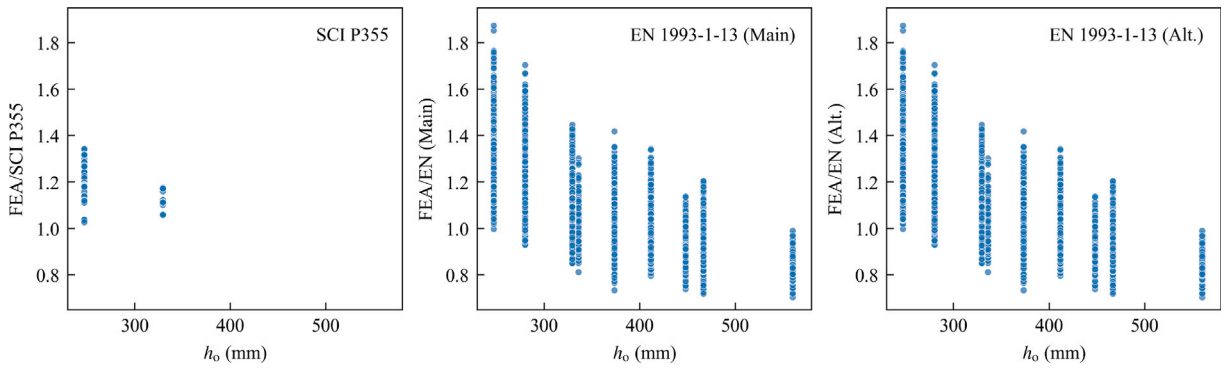

Fig. 11. Effects of h_o on the prediction accuracy for the WPS resistance of cellular beams.

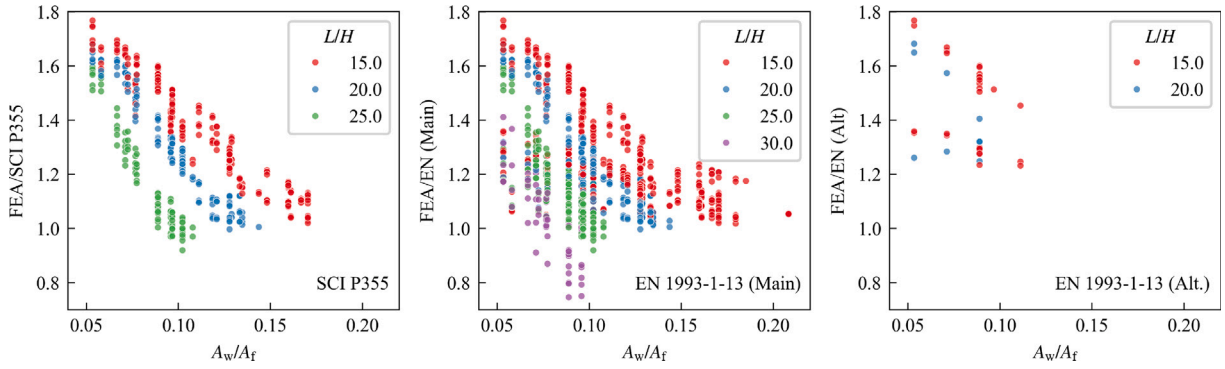

Fig. 12. Effects of A_w/A_f and L/H on the prediction accuracy for the BGS resistance of cellular beams.

Table 2
Statistical properties of random variables.

Properties	Variables	Mean (bias)	CoV	Distribution	Reference
Geometry	H/H_n	1.00	0.009	Lognormal	[24]
	b_f/b_{fn}	1.00	0.009	Lognormal	[24]
	t_w/t_{wn}	1.00	0.025	Lognormal	[24]
	t_f/t_{fn}	0.98	0.025	Lognormal	[24]
	L/L_n	1.00	0.001	Lognormal	[41]
	h_o/h_{on}	1.01	0.006	Lognormal	[41]
	s/s_n	1.00	0.008	Lognormal	[41]
Material	f_y/f_{yn} for f_{yn} = 275 MPa	1.25	0.055	Lognormal	[24]
	f_y/f_{yn} for f_{yn} = 355 MPa	1.20	0.050	Lognormal	[24]
	f_y/f_{yn} for f_{yn} = 460 MPa	1.15	0.045	Lognormal	[24]
	E_s/E_{sn}	1.00	0.030	Lognormal	[24]
Load	D/D_n (US)	1.05	0.100	Normal	[42]
	D/D_n (Europe)	1.00	0.100	Normal	[43]
	L/L_n (US)	1.00	0.250	Gumbel	[42]
	L/L_n (Europe)	0.60	0.350	Gumbel	[43]
Model error	ME	Table 7	Table 7	Lognormal	This study

not overly punish FE simulation-based resistances compared to those from physical testing. It should be noted, however, that the approach of considering FE simulation results as experimental resistance values, without modifying them by an FE model factor, for design model calibration purposes has been used by other researchers [49–52].

Following [50–53], the partial factor, γ_M, required for each beam failure mode predicted by SCI P355 [1] and EN 1993-1-13 [23] was determined from Eq. (9) in accordance with EN 1990 [44] Annex D, which requires a target value of the reliability index for a 50-year reference period of $\beta_{50} = 3.8$.

$$\gamma_M = r_n/r_d, \tag{9}$$

where r_n is the nominal resistance determined from the design provision equations using the nominal geometric and material properties, and r_d is the design resistance determined from Eq. (10).

$$r_d = b g_{rt}\left(\underline{X}_m\right) \exp\left(-k_{d,\infty}\alpha_{rt}Q_{rt} - k_{d,n}\alpha_\delta Q_\delta - 0.5Q^2\right), \tag{10}$$

where $g_{rt}\left(\underline{X}_m\right)$ is the resistance predicted by the design provision equations based on the mean values of the geometric and material properties, with the remaining variables as defined in EN 1990 [44].

The mean values of the geometric and material properties were determined by multiplying their nominal properties by the mean values presented in Table 2, where the subscript n relates to the nominal properties. Table 2 also shows the statistical properties of loads and model error used in Sections 5.2 and 5.3.

The CoV, V_{rt}, was determined from Monte Carlo simulations, considering two approaches: (1) 10,000 random samples for each beam

Table 3
Reliability analysis results for SCI P355 [1] in accordance with EN 1990 [44] Annex D.

Steel grade	Failure mode	n	$k_{d,n}$	b	V_δ	V_{rt}	V_r	γ_M
S275, S355, S460	BGS	492	3.06	1.269	0.158	0.082	0.178	1.19
	BGB	1780	3.05	1.020	0.043	0.065	0.078	1.06
	VBT	567	3.06	1.269	0.209	0.123	0.243	1.60
	WPS	111	3.13	1.178	0.068	0.068	0.096	0.97
	WPB	47	3.25	1.210	0.054	0.069	0.088	1.07
S275	BGS	200	3.09	1.278	0.158	0.079	0.176	1.14
	BGB	687	3.05	1.021	0.032	0.060	0.068	0.99
	VBT	68	3.18	1.147	0.110	0.170	0.202	1.61
	WPS	42	3.28	1.189	0.073	0.062	0.096	0.94
S355	BGS	174	3.09	1.275	0.156	0.075	0.174	1.18
	BGB	557	3.06	1.020	0.040	0.056	0.068	1.03
	VBT	222	3.08	1.273	0.218	0.129	0.254	1.65
	WPS	37	3.31	1.182	0.070	0.058	0.091	0.97
	WPB	9	4.61	1.227	0.030	0.068	0.074	1.01
S460	BGS	118	3.12	1.260	0.162	0.071	0.177	1.26
	BGB	536	3.06	1.020	0.056	0.051	0.076	1.10
	VBT	227	3.07	1.286	0.211	0.101	0.234	1.53
	WPS	32	3.36	1.171	0.058	0.054	0.079	0.98
	WPB	36	3.32	1.209	0.058	0.068	0.090	1.09

generated using traditional random sampling, similar to [54–58]; and (2) 500 random samples for each beam generated using the Latin Hypercube sampling (LHS) technique [59–62]. The latter was needed due to the high computational cost of the reliability analyses for EN 1993-1-13 [23] with the alternative VBT provisions requiring calculations for 660,000 to 2,530,000 sections for each beam, depending on the number of openings, when 10,000 random samples were considered. Comparisons of the results showed an insignificant difference between the V_{rt} and γ_M values produced from the two approaches. Therefore, the results for 500 random LHS samples with the statistical properties from Table 2 are presented in this paper. Moreover, beams with random properties outside the applicability limits of the design provisions were excluded from the analyses.

Separate reliability analyses were conducted for each failure mode, considering all studied steel grades (S275, S355, and S460) and each steel grade separately. Only the beams complying with the applicability limits imposed by each design document (see Section 2) were analyzed.

The results from the reliability analysis are presented in Tables 3, 4, and 5 for SCI P355 [1], EN 1993-1-13 [23] with the main VBT provisions, and EN 1993-1-13 [23] with the alternative VBT provisions, respectively. It should be noted that the results for the SCI P355 [1] case with two beams (see Fig. 6) and the EN 1993-1-13 [23] case with three beams (see Fig. 8) are not presented because $k_{d,n}$ values are too punishing for such small n values.

The reliability analyses for the alternative VBT provisions of EN 1993-1-13 [23] were computationally expensive because multiple radial planes had to be checked for each web opening and the reduced web thickness had to be determined through iterations. To reduce the computational cost, the additional models introduced in the numerical study to ensure an opening at the beam mid-span (see Section 3) and the beams with the intermediate values of the variables considered in the numerical study were excluded from the reliability analyses. This explains the differences between the n values for the VBT failure mode shown in Fig. 8 and those in Table 5.

To enable conclusions to be drawn on the performance of the design provisions with the required target reliability level [24,44], the γ_M values from Tables 3, 4, and 5 should be compared with $\gamma_M = 1.00$ specified in SCI P355 [1], EN 1993-1-13 [23], and EN 1993-1-1 [24] for all failure modes considered in the study.

Table 3 indicates that the γ_M values for the SCI P355 [1] provisions calculated in accordance with EN 1990 [44] Annex D exceed $\gamma_M = 1.00$ specified in Eurocode 3 for all failure modes except for WPS. According to these results, the required partial factors for the BGS, BGB, VBT, and WPB failure modes should be 1.20, 1.05, 1.60, and 1.05, respectively, for steel grades S275, S355, and S460 considered in the study. These recommended values represent the γ_M values for all steel grades from Table 3 rounded to the nearest 0.05.

For EN 1993-1-13 [23] with the main VBT provisions, the required partial factors for all the failure modes exceed 1.00. Table 4 indicates that the γ_M values for the BGS, BGB, VBT, WPS, and WPB failure modes should be 1.20, 1.10, 1.45, 1.35, and 1.60, respectively, for EN 1993-1-13 [23] with the main VBT provisions. The calculated γ_M values for WPS and WPB are significantly higher than those for SCI P355 [1] (1.36 vs. 0.97 and 1.62 vs 1.07, respectively), which is explained by the beams with narrower web-posts permitted by EN 1993-1-13 [23] and a smaller imperfection factor specified by EN 1993-1-13 [23] for WPB (0.21 for buckling curve *a* vs. 0.49 for buckling curve *c* in SCI P355 [1]). The calculated BGB partial factor of 1.09 for EN 1993-1-13 [23] is also slightly higher than SCI P355 [1] (1.06). At the same time, a smaller γ_M value is required for the VBT failure mode in accordance with EN 1993-1-13 [23] than that for SCI P355 [1] (1.47 vs. 1.60). The different γ_M values obtained for the identical requirements for BGB and VBT in EN 1993-1-13 [23] and SCI P355 [1] can be explained by the different number of beams considered in the analyses due to the different applicability limits of these design provisions.

For EN 1993-1-13 [23] with the alternative VBT provisions, only the calculated γ_M values for BGS and BGB meet the Eurocode requirements (see Table 5). The lower BGS partial factor than that required for EN 1993-1-13 [23] with the main VBT provisions is explained by a significantly smaller number of the beams failing in BGS when the alternative VBT method is used (37 vs. 1004). Based on the presented analyses, the recommended γ_M values for VBT, WPS, and WPB are 1.50, 1.35, and 1.65, which are similar to those for EN 1993-1-13 [23] with the main VBT provisions.

5.2. LRFD resistance and ASD safety factors for AISC DG31 [2] in accordance with AISI S100 [45] Chapter K

AISI S100 [45] Chapter K provides a simple equation (Eq. (11)) for calculating the LRFD resistance factor, ϕ, for cold-formed steel (CFS) structures based on statistical properties of the structural member's dimensions, its material properties, and design model error (which are all considered as random variables).

$$\phi = C_\phi (M_m F_m P_m) e^{-\beta_o \sqrt{V_M^2 + V_F^2 + C_P V_P^2 + V_Q^2}}, \tag{11}$$

where C_ϕ is the calibration coefficient that depends on the statistical properties of the live and dead loads and the ratio of the nominal live load, L_n, to the nominal dead load, D_n; M_m and V_M are the mean value and the CoV of material factor, which account for the variability of the material properties; F_m and V_F are the mean value and the CoV of fabrication factor, which account for the variability of the geometric

Table 4
Reliability analysis results for EN 1993-1-13 [23] with the main VBT provisions in accordance with EN 1990 [44] Annex D.

Steel grade	Failure mode	n	$k_{d,n}$	b	V_δ	V_{rt}	V_r	γ_M
S275, S355, S460	BGS	1004	3.05	1.209	0.138	0.082	0.160	1.18
	BGB	4647	3.04	1.024	0.056	0.065	0.086	1.09
	VBT	1415	3.05	1.212	0.182	0.105	0.210	1.47
	WPS	5711	3.04	1.171	0.160	0.081	0.180	1.36
	WPB	777	3.05	1.044	0.118	0.089	0.148	1.62
S275	BGS	408	3.06	1.222	0.135	0.078	0.156	1.11
	BGB	1784	3.05	1.022	0.040	0.060	0.072	1.00
	VBT	168	3.10	1.140	0.100	0.151	0.181	1.46
	WPS	2076	3.04	1.199	0.166	0.076	0.183	1.29
	WPB	82	3.16	0.987	0.072	0.090	0.115	1.54
S355	BGS	357	3.07	1.211	0.139	0.075	0.158	1.18
	BGB	1459	3.05	1.023	0.051	0.055	0.075	1.05
	VBT	561	3.06	1.227	0.190	0.100	0.215	1.45
	WPS	1897	3.04	1.184	0.161	0.073	0.177	1.33
	WPB	244	3.08	1.023	0.113	0.092	0.145	1.64
S460	BGS	239	3.08	1.200	0.141	0.071	0.158	1.24
	BGB	1404	3.05	1.026	0.075	0.050	0.090	1.15
	VBT	686	3.05	1.217	0.186	0.089	0.206	1.46
	WPS	1738	3.05	1.152	0.150	0.070	0.165	1.38
	WPB	451	3.06	1.051	0.118	0.087	0.147	1.61

Table 5
Reliability analysis results for EN 1993-1-13 [23] with the alternative VBT provisions in accordance with EN 1990 [44] Annex D.

Steel grade	Failure mode	n	$k_{d,n}$	b	V_δ	V_{rt}	V_r	γ_M
S275, S355, S460	BGS	37	3.31	1.441	0.114	0.074	0.135	0.92
	BGB	1101	3.05	1.048	0.034	0.061	0.070	1.02
	VBT	812	3.05	1.229	0.175	0.130	0.218	1.48
	WPS	5529	3.04	1.177	0.160	0.081	0.180	1.35
	WPB	696	3.05	1.054	0.129	0.091	0.158	1.67
S275	BGS	25	3.47	1.455	0.114	0.071	0.134	0.91
	BGB	297	3.07	1.038	0.023	0.057	0.062	0.96
	VBT	280	3.07	1.187	0.121	0.122	0.172	1.29
	WPS	2037	3.04	1.203	0.166	0.077	0.183	1.28
	WPB	63	3.20	0.910	0.055	0.079	0.096	1.60
S355	BGS	9	4.61	1.423	0.118	0.068	0.136	1.09
	BGB	396	3.06	1.042	0.031	0.053	0.062	1.00
	VBT	275	3.07	1.244	0.193	0.065	0.204	1.32
	WPS	1828	3.05	1.189	0.160	0.073	0.176	1.33
	WPB	228	3.08	1.024	0.116	0.092	0.148	1.66
S460	BGB	308	3.07	1.055	0.043	0.048	0.065	1.03
	VBT	263	3.08	1.237	0.197	0.164	0.256	1.83
	WPS	1664	3.05	1.158	0.150	0.071	0.165	1.38
	WPB	405	3.06	1.067	0.131	0.090	0.159	1.66

properties; P_m and V_P are the mean value and the CoV of professional factor, which account for the design model error; β_o is the target reliability index; $C_P = (1+1/n)m/(m-2)$ is the correction factor; n is the number of considered samples; $m = n - 1$ are the degrees of freedom; and V_Q is the CoV of load effect.

Eq. (11) is based on the same approach [42,63,64] as that used for developing the LRFD method in AISC 360 [29]. The AISI S100 [45] provisions with the following modifications were used in this study because AISC 360 [29] does not provide a method for determining the LRFD resistance factor based on tests or numerical simulations.

The C_ϕ and V_Q values presented in AISI S100 [45] were derived for $\alpha = L_n/D_n = 5$. This load ratio is appropriate for CFS structures but is too high for hot-rolled steel structures featuring the typical α values ranging from 1.0 to 2.0 [63]. For the purposes of this study, the C_ϕ and V_Q values were recalculated for $\alpha = 1$ and 2, following the method given in AISI S100 Commentary [45] and using the statistical properties of the loads given in Table 2, which gave $C_\phi = 1.37$ and $V_Q = 0.13$ for $L_n/D_n = 1$ and $C_\phi = 1.44$ and $V_Q = 0.17$ for $L_n/D_n = 2$.

$M_m = 1.10$, $V_M = 0.10$, $F_m = 1.00$, and $V_F = 0.05$ were assumed following AISI S100 [45] because these values were also used in the LRFD method calibration for hot-rolled steel structures [42,63,64].

The P_m and V_P values were taken as the mean and the CoV of the simulation-to-prediction ratios for AISC DG31 [2] given in Fig. 9. The target reliability index of 3.00 was used according to [42,63,65].

The ASD safety factor can be determined from the LRFD resistance factor using Eq. (12), which is based on the following ASCE 7 [65] load combination: $1.2D_n+1.6L_n$.

$$\Omega = (1.2 + 1.6\alpha)/[\phi(1 + \alpha)] \tag{12}$$

Table 6 summarizes the n, P_m, and V_P values used in the analyses and presents the most conservative calculated ϕ- and Ω-factors for α ranging from 1 to 2.

Table 6 indicates that the calculated ϕ and Ω values for WPB were more favorable than those specified in AISC DG31 [2] and AISC 360 [29] ($\phi = 0.9$ and $\Omega = 1.67$) indicating that the AISC DG31 [2] provisions satisfy the reliability requirements for WPB. At the same time, the provisions can be considered overly conservative for this failure mode based on the differences between the calculated ϕ and Ω factors and those specified in AISC DG31 [2] and AISC 360 [29].

The analysis results also indicate that the AISC DG31 [2] provisions are not conservative for VBT, as the calculated ϕ and Ω values (0.84 and 1.75) are less favorable than those specified in AISC DG31 [2] and AISC 360 [29] (0.90 and 1.67).

5.3. Improved Hasofer–Lind–Rackwitz–Fiessler (iHL–RF) reliability method analyses

The iHL–RF method [46–48] reliability analyses were performed using Fortuna.jl [66], a general-purpose Julia package for structural

Table 6
Reliability analysis results for AISC DG31 [2] in accordance with AISI S100 [45] Chapter K.

Steel grade	Failure mode	n	P_m	V_P	ϕ	Ω
S275, S355, S460	VBT	5833	1.43	0.263	0.84	1.75
	WPB	5021	1.57	0.155	1.16	1.26
S275	VBT	1933	1.45	0.274	0.82	1.77
	WPB	1685	1.63	0.156	1.20	1.22
S355	VBT	1942	1.43	0.264	0.83	1.75
	WPB	1676	1.57	0.150	1.17	1.25
S460	VBT	1958	1.41	0.251	0.85	1.72
	WPB	1660	1.51	0.148	1.13	1.30

Table 7
Statistical properties of the model error, ME.

Steel	Failure	SCI P355			EN 1993-1-13 (main)			EN 1993-1-13 (alt.)			AISC DG31		
grade	mode	n	Mean	CoV	n	Mean	CoV	n	Mean	CoV	n	Mean	CoV
S275, S355, S460	BGS	246	1.278	0.175	602	1.204	0.140	24	1.459	0.146	0	–	–
	BGB	605	1.020	0.043	2898	1.017	0.052	500	1.044	0.033	0	–	–
	VBT	210	1.316	0.240	886	1.245	0.183	544	1.190	0.178	3643	1.431	0.273
	WPS	54	1.183	0.067	3551	1.086	0.165	3443	1.089	0.165	0	–	–
	WPB	19	1.224	0.055	487	1.023	0.119	427	1.027	0.132	3161	1.570	0.154
S275	BGS	100	1.286	0.181	245	1.215	0.138	15	1.474	0.137	0	–	–
	BGB	231	1.021	0.032	1112	1.018	0.039	130	1.040	0.023	0	–	–
	VBT	26	1.160	0.111	110	1.141	0.101	187	1.136	0.123	1205	1.462	0.359
	WPS	20	1.191	0.072	1290	1.107	0.171	1270	1.109	0.171	0	–	–
	WPB	1	1.140	0.013	51	0.951	0.071	36	0.923	0.053	1063	1.628	0.154
S355	BGS	87	1.280	0.177	215	1.200	0.141	7	1.409	0.112	0	–	–
	BGB	191	1.019	0.039	911	1.016	0.048	206	1.044	0.030	0	–	–
	VBT	77	1.320	0.288	351	1.252	0.188	183	1.221	0.204	1213	1.436	0.288
	WPS	19	1.183	0.069	1180	1.086	0.165	1137	1.090	0.164	0	–	–
	WPB	4	1.235	0.061	151	0.992	0.112	140	0.990	0.115	1055	1.574	0.150
S460	BGS	59	1.263	0.175	142	1.190	0.142	2	1.429	0.097	0	–	–
	BGB	183	1.020	0.055	875	1.018	0.068	164	1.057	0.041	0	–	–
	VBT	107	1.360	0.271	425	1.265	0.190	174	1.216	0.201	1225	1.410	0.255
	WPS	15	1.170	0.056	1081	1.060	0.154	1036	1.062	0.154	0	–	–
	WPB	14	1.228	0.059	285	1.052	0.118	251	1.065	0.132	1043	1.509	0.147

and system reliability analysis. The iHL–RF method is more robust than the EN 1990 [44] Annex D and AISI S100 [45] Chapter K methods because they produce reliability indices considering uncertainty and variability of load effect, material and geometric properties, and design model error.

The analyses were performed as follows. For cellular beams under gravity loads, the limit state function was defined as $G = ME \times R - D - L$, where ME is the model error, calculated based on the comparison of the resistance predictions by the design provisions and the FE simulation results; R is the beam resistance; D and L are the applied dead and live loads, respectively. The statistical properties of the model error, ME, which followed lognormal distribution (see Table 2), are presented in Table 7.

The statistical properties of the beam resistance, R, were obtained from Monte Carlo simulations (MCS) of the beam resistance computed with the design provisions considering the random beam properties from Table 2. Previous studies [67,68] showed that 300 to 500 random samples are sufficient for determining the resistance statistics. Therefore, 500 random samples were generated in this study for each beam using the LHS technique [59–62], which ensures that generated random values represent the real variability of each variable, resulting in a smaller number of samples required for a similar level of accuracy when compared with the traditional random sampling. The obtained resistance histogram for each beam was fitted with the lognormal distribution, which was found appropriate, using Fitter (https://fitter.readthedocs.io/en/latest/), a Python library for fitting probability distributions to data. The beam resistance statistics were obtained from the fitted distributions afterwards.

The dead, D, and live, L, loads followed the statistical properties shown in Table 2. Their nominal values, D_n and L_n, were derived from the nominal beam resistance, R_n, considering the load combinations specified in the respective standards: EN 1990 [44] for both SCI P355 [1] and EN 1993-1-13 [23], and ASCE 7 [65] for AISC DG31 [2], as follows [68].

$$D_n = \phi R_n / (\gamma_D + \gamma_L \alpha) \tag{13}$$

$$L_n = \alpha \phi R_n / (\gamma_D + \gamma_L \alpha). \tag{14}$$

where ϕ is the nominal resistance reduction factor, taken as $1/\gamma_M$ for SCI P355 [1] and EN 1993-1-13 [23], and ϕ and $1/\Omega$ for the AISC DG31 [2] LRFD and ASD methods, respectively; γ_D is the load factor for the dead load (1.35 for the Eurocode framework [44], and 1.2 and 1.0 for the AISC LRFD and ASD methods [65], respectively); γ_L is the load factor for the live load (1.5 for the Eurocode framework [44], and 1.6 and 1.0 the AISC LRFD and ASD methods [65], respectively); and $\alpha = L_n / D_n$.

The iHL–RF method uses the first-order Taylor expansion of the limit state function at a design point on the failure boundary. The design point, unknown *a priori*, is found by iterations based on the negative gradient descent with the step size determined using a line search algorithm. At each iteration, correlated random variables are transformed into an equivalent space of uncorrelated normally distributed variables using the Nataf transformation [48,69]. The reliability index, β, is computed in the equivalent space of uncorrelated normally distributed variables.

Cellular beams with the parameters considered in the numerical study described in Section 3 were analyzed. The web openings were spread evenly along the beam span between the web stiffeners at the beam supports. Subsequently, the beams that did not meet the applicability limits of each design document were excluded. The total number of the beams considered in the iHL–RF method analyses for each steel grade and failure mode, n, are given in Table 7.

The reliability analyses were performed for α values of 0.11, 0.25, 0.50, 1.0, 1.5, and 2.0. The last three values covered the typical range for hot-rolled steel structures [63], while the remaining values were

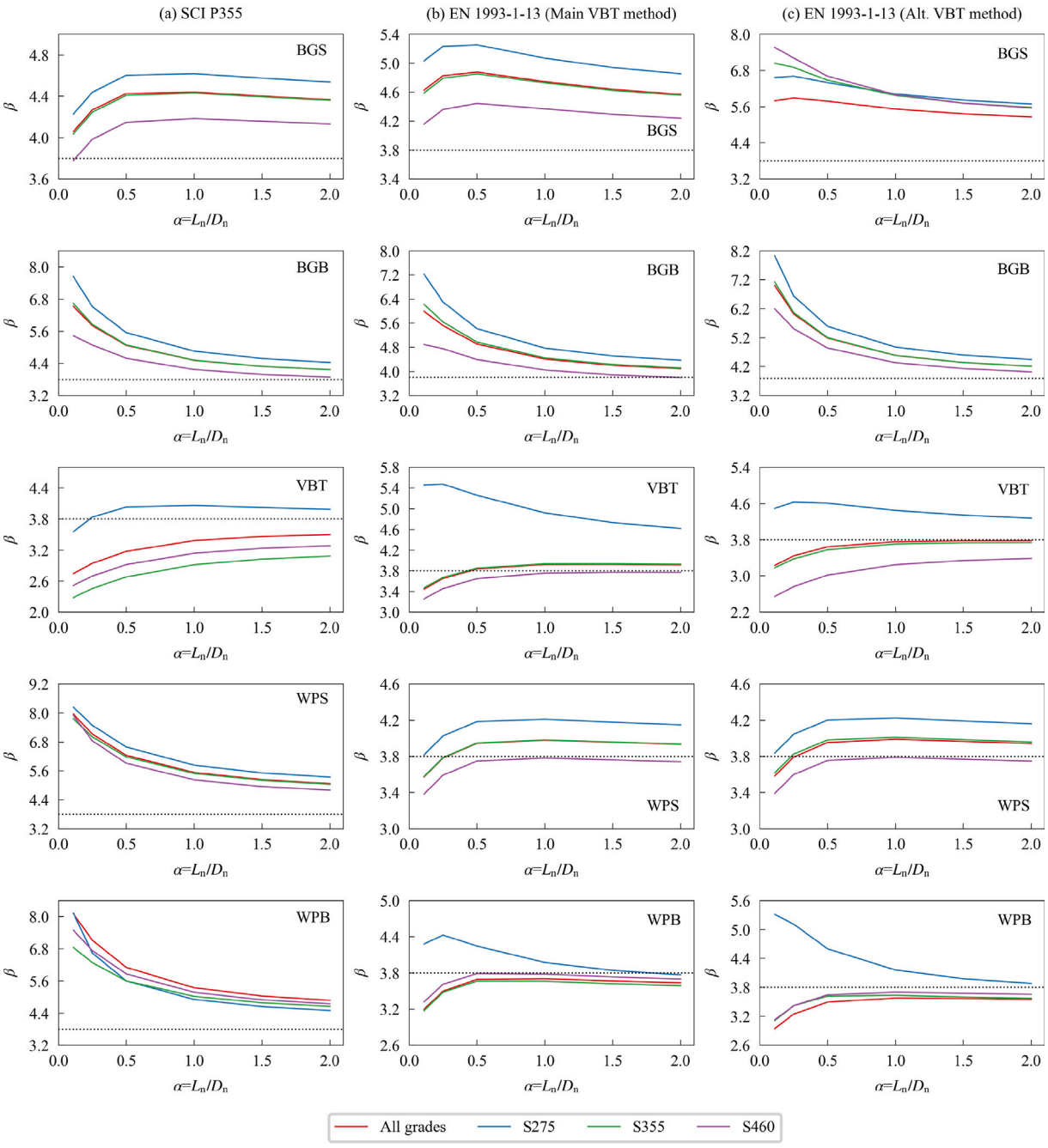

Fig. 13. iHL–RF method analysis results for SCI P355 [1] and EN 1993-1-13 [23].

considered for the completeness of the analyses. The reliability indices produced by the iHL–RF method were compared with target reliability indices of $\beta_{50} = 3.8$ [44] for SCI P355 [1] and EN 1993-1-13 [23] and 3.0 [42,63,65] for AISC DG31 [2].

Figs. 13 and 14 show the computed reliability indices, β, as functions of the load ratio, α for the European provisions (SCI P355 [1] and EN 1993-1-13 [23]) and AISC DG31 [2], respectively. The dotted horizontal lines in Figs. 13 and 14 relate to the target reliability indices.

Fig. 13(a) indicates that the reliability indices for the SCI P355 [1] beam resistances against all failure modes, except for VBT, exceeded $\beta_{50} = 3.8$ for all considered α values. The reliability indices for the VBT resistance of the cellular beams made from steel grades S275 were higher than the target reliability index for α values between 1 and 2, which can be attributed to the relatively small number of the beams exhibiting this failure mode. For the combined steel grades and steel grades S355 and S460 analyzed separately, the reliability indices for the VBT resistance ranged from 2.92 to 3.50, indicating that the SCI P355 [1] design provisions did not satisfy the reliability requirements of EN 1990 [44]. It can also be observed from Fig. 13 that the reliability indices generally decreased when the steel grade increased, which can be explained by the higher mean-to-nominal yield strength ratios for lower steel grades (see Table 2).

Fig. 13(b) shows that the reliability indices predicted by EN 1993-1-13 [23] with the main VBT provisions exceeded the target value of 3.8 for all analyzed cases, except for the WPB resistance of cellular beams of all steel grades and the VBT and WPS resistances of grade S460 beams. The smaller reliability indices for the WPB failure mode according to EN 1993-1-13 [23] than those for SCI P355 [1] are explained by the narrower web-posts and a higher imperfection factor for WPB permitted by EN 1993-1-13 [23]. The narrower web-posts also explain the lower

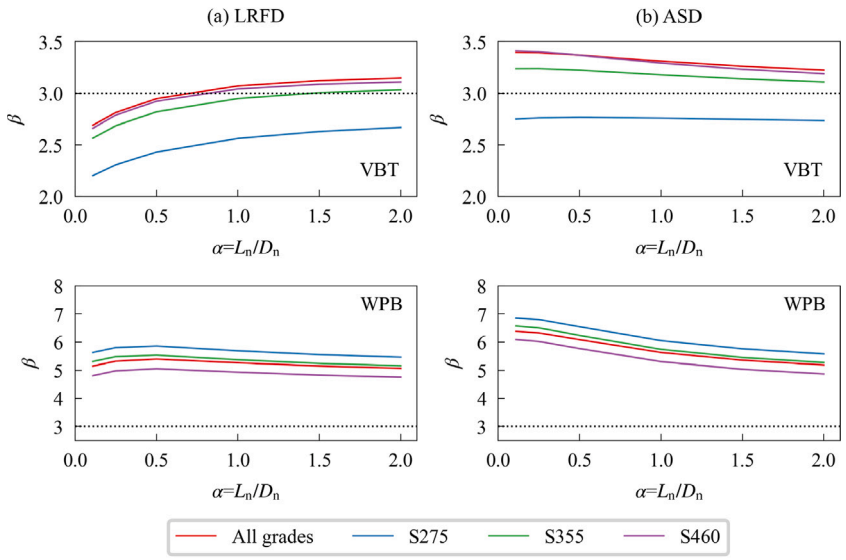

Fig. 14. iHL–RF method analysis results for AISC DG31 [2].

β values for the WPS failure mode. The reliability indices for the VBT resistance in accordance with the main method of EN 1993-1-13 [23] are 12% to 35% higher than those determined for SCI P355 [1]. Because the VBT provisions in both design documents are identical, this difference in the VBT reliability indices can be attributed to a broader scope of EN 1993-1-13 [23] and the larger number of beams analyzed for it (see Table 7).

The reliability analysis results for EN 1993-1-13 [23] with the alternative VBT provisions presented in Fig. 13(c) indicate that the calculated β values were smaller than the target reliability index of 3.8 for α between 1 and 2 for the following cases: VBT and WPB for all steel grades, S355 and S460, and WPS for steel grade S460. The VBT reliability indices for the alternative VBT method were reduced by 3% to 14%, depending on the steel grade, when compared with the main VBT method. For all steel grades, the reliability index reductions were approximately 4%. These results indicate that the alternative VBT method is slightly less conservative than the main VBT method. The differences between the reliability indices for the main and alternative VBT methods for failure modes other than VBT are explained by the different number of beams considered in the analyses (see Table 7).

Fig. 14 shows that the cellular beam design in accordance with AISC DG31 [2] produced reliability indices higher than the target value of 3.0 for all considered cases, except for the VBT failure mode of the beams made from steel grades S275 and S355 designed using LRFD and from steel grade S275 designed using ASD. For WPB, AISC DG31 [2] produced reliability indices considerably higher than the required target value of 3.0, indicating significant conservatism of the provisions in predicting the beam resistance governed by WPB. It can also be noted that ASD produced higher reliability indices than LRFD. The reliability indices decreased when the steel grade increased for WPB, while the opposite was true for VBT.

For the cases where the considered design provisions produced reliability indices smaller than the target values, the γ_M, ϕ, and Ω values required to achieve the target reliability indices were determined with the iHL–RF method. Table 8 summarizes the obtained results.

A comparison of the required partial factors from Table 8 with those presented in Section 5.1 shows that the iHL–RF method produced smaller required γ_M values than those based on EN 1990 [44] Annex D in all cases. For AISC DG31 [2], the VBT ϕ and Ω factors determined using the iHL–RF method were more favorable than those computed in Section 5.2 in all cases, except for steel grade S275.

Considering that the iHL–RF method is more robust than those used in Sections 5.1 and 5.2, the calculated reduction factor values given in Table 8 are recommended for design.

6. Discussion of the results and future research directions

The results of the presented study indicate that the European design provisions predict the resistance of laterally restrained steel beams with reasonable accuracy, characterized by the following mean RRs and their CoVs: 1.13 and 0.185 for SCI P355 [1]; 1.08 and 0.158 for EN 1993-1-13 [23] with the main VBT provisions; and 1.12 and 0.169 for EN 1993-1-13 [23] with the alternative VBT provisions. The resistance predictions for the BGB and WPB failure modes were significantly more accurate than those for the BGS, VBT, and WPS failure modes. The North American AISC DG31 [2] produced considerably higher mean and CoV of the RRs of 1.50 and 0.220, respectively, than the European design documents.

It was found that the accuracy of the European provisions can be improved as follows. The VBT resistance predictions can be improved by refining the equivalent opening size in the main VBT method to account for the nonlinear effect of the web opening diameter on the VBT resistance instead of the current linear relationship. Implementing the opening diameter effect into the WPS resistance calculations, in addition to it simply affecting the web-post width in the current design documents, should improve the WPS resistance accuracy. Finally, accounting for the beam flange contribution to the BGS resistance and considering the moment gradient effect should make the BGS predictions more accurate. The accuracy of AISC DG31 [2] can be improved by adopting the WPB provisions similar to those in EN 1993-1-13 [23] and modifying the VBT provision as discussed above for the European standard.

The reliability assessments showed that partial factors higher than 1.00, specified in the current Eurocodes, are required for many failure modes to meet the Eurocode reliability requirements when the partial factors are determined in accordance with EN 1990 [44] Annex D. However, more robust reliability evaluations using the iHL–RF method produced more favorable partial factor values, justifying $\gamma_M = 1.00$ for all limit states in EN 1993-1-13 [23] when steel grades S275, S355, and S460 are considered together (except for WPB where $\gamma_M = 1.05$ is required). For North American AISC DG31 [2], currently used $\phi = 0.90$ and $\Omega = 1.67$ were justified for the VBT and WPB failure modes by the analysis results using the iHL–RF method, whereas the AISI S100 [45] Chapter K method produced less favorable ϕ and Ω values for VBT.

The presented study also found that the prediction accuracy of the WPB resistance in accordance with EN 1993-1-13 [23], which uses the EN 1993-1-1 [24] buckling curve *a*, is better than that in accordance with SCI P355 [1] (which employs buckling curve *c*). However, the

Table 8
Required reduction factors based on the iHL–RF method analyses.

Steel grade	Failure mode	γ_M			ϕ	Ω
		SCI P355	EN 1993-1-13 (main)	EN 1993-1-13 (alt.)	AISC DG31	
S275, S355, S460	BGS	1.00	1.00	1.00	–	–
	BGB	1.00	1.00	1.00	–	–
	VBT	1.12	1.00	1.01	0.90	1.67
	WPS	1.00	1.00	1.00	–	–
	WPB	1.00	1.04	1.06	0.90	1.67
S275	BGS	1.00	1.00	1.00	–	–
	BGB	1.00	1.00	1.00	–	–
	VBT	1.00	1.00	1.00	0.76	1.85
	WPS	1.00	1.00	1.00	–	–
	WPB	1.00	1.01	1.00	0.90	1.67
S355	BGS	1.00	1.00	1.00	–	–
	BGB	1.00	1.00	1.00	–	–
	VBT	1.33	1.00	1.03	0.88	1.67
	WPS	1.00	1.00	1.00	–	–
	WPB	1.00	1.05	1.05	0.90	1.67
S460	BGS	1.00	1.00	1.00	–	–
	BGB	1.00	1.00	1.00	–	–
	VBT	1.22	1.02	1.15	0.90	1.67
	WPS	1.00	1.02	1.02	–	–
	WPB	1.00	1.03	1.04	0.90	1.67

higher prediction accuracy and CoV compared with SCI P355 [1] comes at a cost, in that the reliability of the EN 1993-1-13 [23] WPB provisions do not satisfy the target value of the reliability index required by EN 1990 [44]. Therefore, a more onerous buckling curve should be adopted for the WPB design model given in this standard.

As opposed to EN 1993-1-13 [23], given that AISC DG31 [2] does not require high shear forces to be accounted for within the VBT resistance calculations, the effects of the web thickness reduction due to high shear forces on the accuracy and reliability of the Eurocode predictions were evaluated. The web thickness reduction affected 709 (23.7%), 3140 (23.2%), and 6446 (47.6%) beams for SCI P355 [1], EN 1993-1-13 [23] with the main VBT provisions, and EN 1993-1-13 [23] with the alternative VBT provisions, respectively. The maximum resistance reductions for these provisions were 15.9%, 25.2%, and 25.9%, respectively. However, the average resistance reductions due to high shear for all considered beams were relatively small: 0.3%, 0.2%, and 1.4% for SCI P355 [1], EN 1993-1-13 [23] with the main VBT provisions, and EN 1993-1-13 [23] with the alternative VBT provisions, respectively. For all steel grades, the mean VBT RR values increased by 5% and 2% for SCI P355 [1] and EN 1993-1-13 [23] with the main VBT provisions and decreased by 4% for EN 1993-1-13 [23] with the alternative VBT provisions when the t_w reduction was neglected. The mean VBT RR increases were caused by the different number of beams showing the VBT failure mode after accounting for the t_w reduction. At the same time, the CoVs of the VBT RRs increased by 10%, 12%, and 1% for these three provisions. The required partial factors for the VBT resistance with the t_w reduction neglected either increased or reduced slightly for different provisions compared with those considering the t_w reduction.

It was also found that each failure mode's accuracy and reliability assessment results depended on the number of considered beams, which were affected by the applicability limits and relative conservatism of the resistance predictions for each limit state. More conservative resistance predictions for one failure mode than the others resulted in more beams assigned to it (indicating that it is more probable), affecting the accuracy and reliability assessment results for that and other failure modes. Therefore, the accuracy and reliability assessments should be performed considering the interactions between the limit states (failure modes).

7. Conclusions

This study introduced an extensive database of FE simulation results for laterally restrained cellular steel beams under uniform loads and evaluated the accuracy and reliability of SCI P355 [1], EN 1993-1-13 [23], and AISC DG31 [2] in predicting the resistance. Such accuracy and reliability assessments have not been reported previously.

The database, covering a wide range of beam parameters used in construction, was developed using geometrically and materially nonlinear FE models that accounted for the initial geometric imperfections and residual stresses. The FE models were validated against ten test results to show good prediction accuracy, which was characterized by test-to-simulation ratios ranging from 0.96 to 1.03, with a mean value of 0.99 and a CoV of 0.022.

A numerical parametric study based on the developed FE models demonstrated that the beams exhibited various failure modes, including BGS, BGB, VBT, WPS, and WPB, with many failure mode interactions. The elimination of the LTB failure mode through the provision of lateral restraints allowed beam resistances governed by other failure modes to be obtained for the beams spanning up to $30H$. The effects of the studied parameters, such as H, b_f, t_w, t_f, L/H, H/h_o, s/h_o, and f_y, on the beam resistance were presented and discussed.

The accuracy assessment indicated that SCI P355 [1] and EN 1993-1-13 [23] predicted the beam resistance reasonably well, with EN 1993-1-13 [23] and the main VBT provisions being slightly more accurate than the others for all considered steel grades and failure modes. On the other hand, AISC DG31 [2] produced significantly higher mean value and CoV of the RRs than those for the European design documents.

It was also found that employing EN 1993-1-1 [24] buckling curve *a*, specified in EN 1993-1-13 [23] resulted in more accurate WPB resistance predictions when compared with buckling curve *c* required by SCI P355 [1]. Additionally, relatively large scatters of the simulation-to-prediction ratios were observed for the BGS failure mode and WPS failure mode for the beams with $0.3h_o \geq s_o \geq 0.1h_o$, while the BGB resistance predictions by SCI P355 [1] and EN 1993-1-13 [23] were accurate.

The beam parameters affecting the prediction accuracy of the VBT, WPS, and BGS resistances, whose scatters were larger than those for BGB and WPB, were investigated, and possible directions for potential accuracy improvements were presented.

The reliability of the existing design provisions was evaluated in accordance with EN 1990 [44] Annex D for both SCI P355 [1] and EN 1993-1-13 [23], and AISI S100 [45] Chapter K with appropriate modifications for AISC DG31 [2]. Reliability analyses using the iHL–RF method [48], considering various live-to-dead load ratios, were also performed for all evaluated design provisions.

The reliability analysis results for SCI P355 [1] and EN 1993-1-13 [23] demonstrated that the predictions of the beam resistance for many failure modes were unconservative in accordance with the EN 1990 [44] Annex D method. However, the iHL–RF method results indicated that $\gamma_M = 1.00$ is justified for all failure modes except for WPB, which requires $\gamma_M = 1.05$ to meet the target value of the reliability index for a 50-year reference period of $\beta_{50} = 3.8$ [44].

Although the resistance predictions were more accurate when compared with the database results, it was found that the reliability of the EN 1993-1-13 [23] WPB provisions did not comply with the Eurocode requirements; conversely, the SCI P355 [1] WPB provisions satisfied these requirements. Based on the reliability analyses, it is recommended that EN 1993-1-13 is revised to require that EN 1993-1-1 [24] buckling curve *c* is used for WPB resistance predictions.

The reliability of the AISC DG31 [2] predictions meets the code requirements for the VBT and WPB failure modes. For the latter, safety margins were large, indicating a possibility for making the design less conservative and more economical.

It was found that the robust iHL–RF method provided more favorable reliability analysis results when compared with the simplified method of EN 1990 [44] Annex D.

The presented results highlight the areas where the existing design provisions need revisions and provide insights on how the improvements can be made, which, when made, will contribute to the safety and economy of construction with cellular steel beams.

CRediT authorship contribution statement

Vitaliy V. Degtyarev: Writing – review & editing, Writing – original draft, Visualization, Validation, Software, Methodology, Investigation, Formal analysis, Data curation, Conceptualization. **Stephen J. Hicks:** Writing – review & editing, Validation, Methodology, Data curation, Conceptualization. **Felipe Piana Vendramell Ferreira:** Writing – review & editing, Validation, Methodology, Data curation. **Konstantinos Daniel Tsavdaridis:** Writing – review & editing, Methodology, Data curation, Conceptualization.

Declaration of competing interest

The authors declare that they have no known competing financial interests or personal relationships that could have appeared to influence the work reported in this paper.

Acknowledgments

The authors would like to express their gratitude to Damir Akchurin, a Ph.D. student at Johns Hopkins University, for developing the Fortuna.jl [66] package and making it publicly available, as well as for his invaluable assistance in using it. The second author acknowledges with thanks the financial support provided by the European Commission/European Free Trade Association under Grant Agreement SA/CEN/GROW/EFTA/515/2017-08 during his period as a member of Project Team CEN/TC 250/SC4.T6.

Data availability

I have shared the link to my data in the following link.

Database of the uniform ultimate loads applied to laterally restrained cellular steel beams (Original data) (Mendeley Data)

References

[1] R. Lawson, S. Hicks, Design Of Composite Beams with Large Web Openings SCI P355, Steel Construction Institute, Berkshire, UK, 2011.
[2] S. Fares, J. Coulson, D. Dinehart, Design Guide 31: Castellated and Cellular Beam Design, American Institute of Steel Construction, Chicago, IL, USA, 2016.
[3] J. Warren, Ultimate Load and Deflection Behaviour of Cellular Beams (Ph.D. thesis), University of Natal, Durban, South Africa, 2001.
[4] C. Müller, O. Hechler, A. Bureau, D. Bitar, D. Joyeux, L. Cajot, T. Demarco, R. Lawson, S. Hicks, P. Devine, O. Lagerqvist, E. Hedman-Pétursson, E. Unosson, M. Feldmann, Large Web Openings for Service Integration in Composite Floors, Report EUR 21345, 2006.
[5] F. Erdal, M.P. Saka, Ultimate load carrying capacity of optimally designed steel cellular beams, J. Constr. Steel Res. 80 (2013) 355–368, http://dx.doi.org/10.1016/j.jcsr.2012.10.007.
[6] L. Kang, S. Hong, X. Liu, Shear behaviour and strength design of cellular beams with circular or elongated openings, Thin-Walled Struct. 160 (2021) 107353, http://dx.doi.org/10.1016/j.tws.2020.107353.
[7] K.D. Tsavdaridis, C. D'Mello, Web buckling study of the behaviour and strength of perforated steel beams with different novel web opening shapes, J. Constr. Steel Res. 67 (10) (2011) 1605–1620, http://dx.doi.org/10.1016/j.jcsr.2011.04.004.
[8] L.F. Grilo, R.H. Fakury, A.L.R. de Castro e Silva, G.d. Veríssimo, Design procedure for the web-post buckling of steel cellular beams, J. Constr. Steel Res. 148 (2018) 525–541, http://dx.doi.org/10.1016/j.jcsr.2018.06.020.
[9] S.G. Morkhade, L.M. Gupta, An experimental and parametric study on steel beams with web openings, Int. J. Adv. Struct. Eng. (IJASE) 7 (3) (2015) 249–260, http://dx.doi.org/10.1007/s40091-015-0095-4.
[10] J. Nseir, M. Lo, D. Sonck, H. Somja, O. Vassart, N. Boissonnade, Lateral torsional buckling of cellular steel beams, in: Structural Stability Research Council Annual Stability Conference, SSRC2012, Grapevine, TX, USA, 2012.
[11] D. Sonck, Global Buckling of Castellated and Cellular Steel Beams and Columns (Ph.D. thesis), Ghent University, Ghent, Belgium, 2014.
[12] K. Rajana, K.D. Tsavdaridis, E. Koltsakis, Elastic and inelastic buckling of steel cellular beams under strong-axis bending, Thin-Walled Struct. 156 (2020) 106955, http://dx.doi.org/10.1016/j.tws.2020.106955.
[13] A. Jamadar, P. Kumbhar, Parametric study of castellated beam with circular and diamond shaped openings, Int. Res. J. Eng. Technol. 2 (2) (2015) 715–722, http://dx.doi.org/10.1016/j.tws.2020.106955.
[14] A.M. Sweedan, Elastic lateral stability of I-shaped cellular steel beams, J. Constr. Steel Res. 67 (2) (2011) 151–163, http://dx.doi.org/10.1016/j.jcsr.2010.08.009.
[15] M.I.M.H. Martini, Elasto-Plastic Lateral Torsional Buckling of Steel Beams with Perforated Web (Ph.D. thesis), United Arab Emirates University, 2011.
[16] D. Sonck, J. Belis, Lateral–torsional buckling resistance of cellular beams, J. Constr. Steel Res. 105 (2015) 119–128, http://dx.doi.org/10.1016/j.jcsr.2014.11.003.
[17] P. Panedpojaman, W. Sae-Long, T. Chub-uppakarn, Cellular beam design for resistance to inelastic lateral–torsional buckling, Thin-Walled Struct. 99 (2016) 182–194, http://dx.doi.org/10.1016/j.tws.2015.08.026.
[18] F.P.V. Ferreira, A. Rossi, C.H. Martins, Lateral-torsional buckling of cellular beams according to the possible updating of EC3, J. Constr. Steel Res. 153 (2019) 222–242, http://dx.doi.org/10.1016/j.jcsr.2018.10.011.
[19] P. Panedpojaman, T. Thepchatri, S. Limkatanyu, Novel design equations for shear strength of local web-post buckling in cellular beams, Thin-Walled Struct. 76 (2014) 92–104, http://dx.doi.org/10.1016/j.tws.2013.11.007.
[20] E. Ellobody, Nonlinear analysis of cellular steel beams under combined buckling modes, Thin-Walled Struct. 52 (2012) 66–79, http://dx.doi.org/10.1016/j.tws.2011.12.009.
[21] J. Ward, Design of Composite and Non-Composite Cellular Beams SCI P100, Steel Construction Institute, Berkshire, UK, 1990.
[22] ENV 1993-1-1: 1992/A2: 1998, Eurocode 3: Design of Steel Structures — Part 1-1: General rules — General Rules and Rules for Buildings - Amendment A2, European Committee for Standardization, Brussels, Belgium, 1998.
[23] EN 1993-1-13, Eurocode 3: Design of Steel Structures - Part 1-13: Rules for Beams with Large Web Openings, European Committee for Standardization, Brussels, Belgium, 2024.
[24] EN 1993-1-1, Eurocode 3 - design of steel structures - part 1-1: General rules and rules for buildings, European Committee for Standardization, Brussels, Belgium, 2022.
[25] P. Panedpojaman, W. Sae-Long, Accuracy of available methods to evaluate Vierendeel failure load, in: Transactions on Engineering Technologies: World Congress on Engineering 2014, Springer, 2015, pp. 163–175, http://dx.doi.org/10.1007/978-94-017-9804-4_11.
[26] V. Akrami, S. Erfani, Review and assessment of design methodologies for perforated steel beams, J. Struct. Eng. 142 (2) (2016) 04015148, http://dx.doi.org/10.1061/(ASCE)ST.1943-541X.0001421.
[27] F.P.V. Ferreira, C.H. Martins, LRFD for lateral-torsional buckling resistance of cellular beams, Int. J. Civ. Eng. 18 (3) (2020) 303–323, http://dx.doi.org/10.1007/s40999-019-00474-7.

[28] EN 1993-1-5, Eurocode 3: Design of steel structures - Part 1-5: Plated Structural Elements, European Committee for Standardization, Brussels, Belgium, 2024.
[29] ANSI/AISC 360-22, Specification for Structural Steel Buildings, American Institute of Steel Construction, Chicago, Illinois, USA, 2022.
[30] P.-O. Martin, Private Communication, CTICM, Saint Aubin, France, 2024.
[31] prEN 1993-1-14, Eurocode 3: Design of steel structures - Part 1-14: Design Assisted by Finite Element Analysis, European Committee for Standardization, Brussels, Belgium, 2023.
[32] D. Sonck, R. Van Impe, J. Belis, Experimental investigation of residual stresses in steel cellular and castellated members, Constr. Build. Mater. 54 (2014) 512–519, http://dx.doi.org/10.1016/j.conbuildmat.2013.12.045.
[33] S. European Convention for Constructional Steelwork. Technical Committee 8, Ultimate Limit State Calculation of Sway Frames with Rigid Joints, ECCS General Secretariat, 1984.
[34] D. Beg, L. Hladnik, Slenderness limit of Class 3 I cross-sections made of high strength steel, J. Constr. Steel Res. 38 (3) (1996) 201–217, http://dx.doi.org/10.1016/0143-974X(96)00025-9.
[35] A. Taras, Contribution to the Development of Consistent Stability Design Rules for Steel Members (Ph.D. thesis), Graz University of Technology, Graz, Austria, 2010.
[36] K.E. Barth, D.W. White, Finite element evaluation of pier moment-rotation characteristics in continuous-span steel I girders, Eng. Struct. 20 (8) (1998) 761–778, http://dx.doi.org/10.1016/S0141-0296(97)00087-4.
[37] V.M. de Oliveira, L.M.S. Prates, A. Rossi, J.P. Martins, L.A.P. Simões da Silva, C.H. Martins, Comparative analysis of geometric imperfections and residual stresses on the global stability behavior of cantilever composite alveolar beams, Structures 65 (2024) 106634, http://dx.doi.org/10.1016/j.istruc.2024.106634.
[38] EN 10025-2, Hot Rolled Products of Structural Steels - Part 2: Technical Delivery Conditions for Non-Alloy Structural Steels, European Committee for Standardization, Brussels, Belgium, 2019.
[39] V.V. Degtyarev, S.J. Hicks, F.P.V. Ferreira, K.D. Tsavdaridis, Database of the uniform ultimate loads applied to laterally restrained cellular steel beams, V.2, 2024, http://dx.doi.org/10.17632/zcm29bp7yf.2, Mendeley Data.
[40] D. Chicco, M.J. Warrens, G. Jurman, The coefficient of determination R-squared is more informative than SMAPE, MAE, MAPE, MSE and RMSE in regression analysis evaluation, PeerJ Comput. Sci. 7 (2021) e623.
[41] EN 1090-2, Execution of Steel Structures and Aluminium Structures - Part 2: Technical Requirements for Steel Structures, European Committee for Standardization, Brussels, Belgium, 2018.
[42] T.V. Galambos, Load and resistance factor design, AISC Eng. J. 18 (3) (1981) 74–82.
[43] H. Gulvanessian, M. Holicky, Eurocodes: using reliability analysis to combine action effects, Proc. Inst. Civ. Eng.-Struct. Build. 158 (4) (2005) 243–252, http://dx.doi.org/10.1680/stbu.2005.158.4.243.
[44] EN 1990:2002+A1, Eurocode: Basis of Structural Design, European Committee for Standardization, Brussels, Belgium, 2005.
[45] ANSI/AISI S100-16 (R2020) w/S3-22, North American Specification for the Design of Cold-Formed Steel Structural Members, American Institute of Steel Construction, Chicago, Illinois, USA, 2022.
[46] A.M. Hasofer, N.C. Lind, Exact and invariant second-moment code format, J. Eng. Mech. Div. 100 (1) (1974) 111–121, http://dx.doi.org/10.1061/JMCEA3.000184.
[47] R. Rackwitz, B. Flessler, Structural reliability under combined random load sequences, Comput. Struct. 9 (5) (1978) 489–494, http://dx.doi.org/10.1016/0045-7949(78)90046-9.
[48] A. Der Kiureghian, Structural and System Reliability, Cambridge University Press, 2022.
[49] J. Gomes Jr., H. Carvalho, L.S. da Silva, J. Ferreira Filho, A. Lavall, Assessment of design procedures for the buckling resistance of hot-rolled steel equal leg angles under concentric and eccentric compression, Structures 57 (2023) 105308, http://dx.doi.org/10.1016/j.istruc.2023.105308.
[50] X. Meng, L. Gardner, Testing, modelling and design of normal and high strength steel tubular beam-columns, J. Constr. Steel Res. 183 (2021) 106735, http://dx.doi.org/10.1016/j.jcsr.2021.106735.
[51] B. Behzadi-Sofiani, L. Gardner, M.A. Wadee, Behaviour, finite element modelling and design of cruciform section steel columns, Thin-Walled Struct. 182 (2023) 110124, http://dx.doi.org/10.1016/j.tws.2022.110124.
[52] X. Yun, Y. Zhu, X. Meng, L. Gardner, Welded steel I-section columns: residual stresses, testing, simulation and design, Eng. Struct. 282 (2023) 115631, http://dx.doi.org/10.1016/j.engstruct.2023.115631.
[53] S. Afshan, P. Francis, N. Baddoo, L. Gardner, Reliability analysis of structural stainless steel design provisions, J. Constr. Steel Res. 114 (2015) 293–304, http://dx.doi.org/10.1016/j.jcsr.2015.08.012.
[54] S.J. Hicks, Design shear resistance of headed studs embedded in solid slabs and encasements, J. Constr. Steel Res. 139 (2017) 339–352, http://dx.doi.org/10.1016/j.jcsr.2017.09.018.
[55] V.V. Degtyarev, S.J. Hicks, J.F. Hajjar, Design models for predicting shear resistance of studs in solid concrete slabs based on symbolic regression with genetic programming, Steel Compos. Struct. 43 (3) (2022) 293–309, http://dx.doi.org/10.12989/scs.2022.43.3.293.
[56] V.V. Degtyarev, S.J. Hicks, Reliability-based design shear resistance of headed studs in solid slabs predicted by machine learning models, Architect. Struct. Construct. (2022) 1–27, http://dx.doi.org/10.1007/s44150-022-00078-1.
[57] V.V. Degtyarev, S.J. Hicks, Shear resistance of welded studs in deck slab ribs transverse to beams, Eng. Struct. 294 (2023) 116709, http://dx.doi.org/10.1016/j.engstruct.2023.116709.
[58] V.V. Degtyarev, S.J. Hicks, Machine learning-based probabilistic predictions of shear resistance of welded studs in deck slab ribs transverse to beams, Steel Compos. Struct. 49 (1) (2023) 109–123, http://dx.doi.org/10.12989/scs.2023.49.1.109.
[59] M.D. McKay, R.J. Beckman, W.J. Conover, A comparison of three methods for selecting values of input variables in the analysis of output from a computer code, Technometrics 42 (1) (2000) 55–61, http://dx.doi.org/10.2307/1268522.
[60] V. Eglajs, P. Audze, New approach to the design of multifactor experiments, Prob. Dyn. Strengths 35 (1) (1977) 104–107.
[61] R.L. Iman, J.C. Helton, J.E. Campbell, An approach to sensitivity analysis of computer models: Part I—Introduction, input variable selection and preliminary variable assessment, J. Qual. Technol. 13 (3) (1981) 174–183, http://dx.doi.org/10.1080/00224065.1981.11978748.
[62] R.L. Iman, J.M. Davenport, D.K. Zeigler, Latin Hypercube Sampling (Program User's Guide).[LHC, in FORTRAN], Tech. Rep., Sandia Labs., Albuquerque, NM (USA, 1980.
[63] B. Ellingwood, B. Galambos, J. MacGregor, C. Cornell, Development of a probability based load criterion for American National Standard A58: Building code requirements for minimum design loads in buildings and other structures, vol. 577, Department of Commerce, National Bureau of Standards, 1980.
[64] M. Ravindra, T. Galambos, Load and resistance factor design for steel, J. Struct. Div. 104 (9) (1978) 1337–1353, http://dx.doi.org/10.1061/JSDEAG.0004981.
[65] ASCE/SEI 7-22, Minimum Design Loads and Associated Criteria for Buildings and Other Structures, American Society of Civil Engineers, Reston, VA, USA, 2022.
[66] D. Akchurin, Fortuna.jl: Structural and system reliability analysis in Julia, J. Open Sour. Softw. 9 (100) (2024) 6967, http://dx.doi.org/10.21105/joss.06967.
[67] R.E. Melchers, A.T. Beck, Structural Reliability Analysis and Prediction, John Wiley & Sons, 2018.
[68] V.V. Degtyarev, H.-T. Thai, Design of concrete-filled steel tubular columns using data-driven methods, J. Constr. Steel Res. 200 (2023) 107653, http://dx.doi.org/10.1016/j.jcsr.2022.107653.
[69] A. Nataf, Détermination des distribution dont les Marges sont Données, C. R Acad. Sci. 225 (1962) 42–43.